B. Deng, *Conceptual circuit models of neurons,* Journal of Integrative Neuroscience, **8**(2009), pp.255–297.

Conceptual Circuit Models of Neurons

Bo Deng[1]

Abstract: A systematic circuit approach to model neurons with ion pump is presented here by which the voltage-gated current channels are modeled as conductors, the diffusion-induced current channels are modeled as negative resistors, and the one-way ion pumps are modeled as one-way inductors. The newly synthesized models are different from the type of models based on Hodgkin-Huxley (HH) approach which aggregates the electro, the diffusive, and the pump channels of each ion into one conductance channel. We show that our new models not only recover many known properties of the HH type models but also exhibit some new that cannot be extracted from the latter.

1. Introduction. The field of mathematical modeling of neurons has seen a tremendous growth ([13, 21, 20, 1, 19, 15]) since the landmark work, [16], of Hodgkin and Huxley on the electrophysiology of neurons. Basic mathematics of these Hodgkin-Huxley (HH) type models are well-understood today ([23]). By the HH approach, mechanistically different current channels of each ion species are aggregated into one conductance-based current. A given ion's distinct pathways through the cell wall can be of the following kinds: the passive channel due to the electromagnetic force of all ions, the passive channel due to the diffusive force against its own concentration gradient across the cell membrane, and the active channel from the ion's one-way ion pump if any. Although the electrophysiological narratives of these channels have been widely known for some time ([17, 24]), no one has attempted to model them individually as elementary circuit elements in a whole circuit synthesis. Also, from a circuit theoretical viewpoint, the HH type models are phenomenological beyond their usage of Kirchhoff's Current Law for the transmembrane currents of all ions, and as a result they are not readily accessible to elementary circuit implementation.

The purpose of this paper is to fill this literature gap. We will start with a generic conceptual model of neurons, deconstruct each ion current into its passive (electric and diffusive) currents and its active (ion pump) current, and then model each channel according to its hypothesized circuit characteristic. We will demonstrate that our newly synthesized models recover many well-known neural dynamics, but cast in the context of their distinctive passive and active channels. Some properties completely unknown to HH type models will be reported in a second paper ([12]).

2. Mathematical Models. Our proposed circuit models are not for a specific type of neurons *per se* but rather for a conceptual embodiment of circuit principles derived from neurophysiology. The models are minimal in the sense that they contains sharply contrasting types of ion species with little duplication of each other's functionalities. But the method is sufficiently general to

[1]Department of Mathematics, University of Nebraska-Lincoln, Lincoln, NE 68588. Email: bdeng1@math.unl.edu

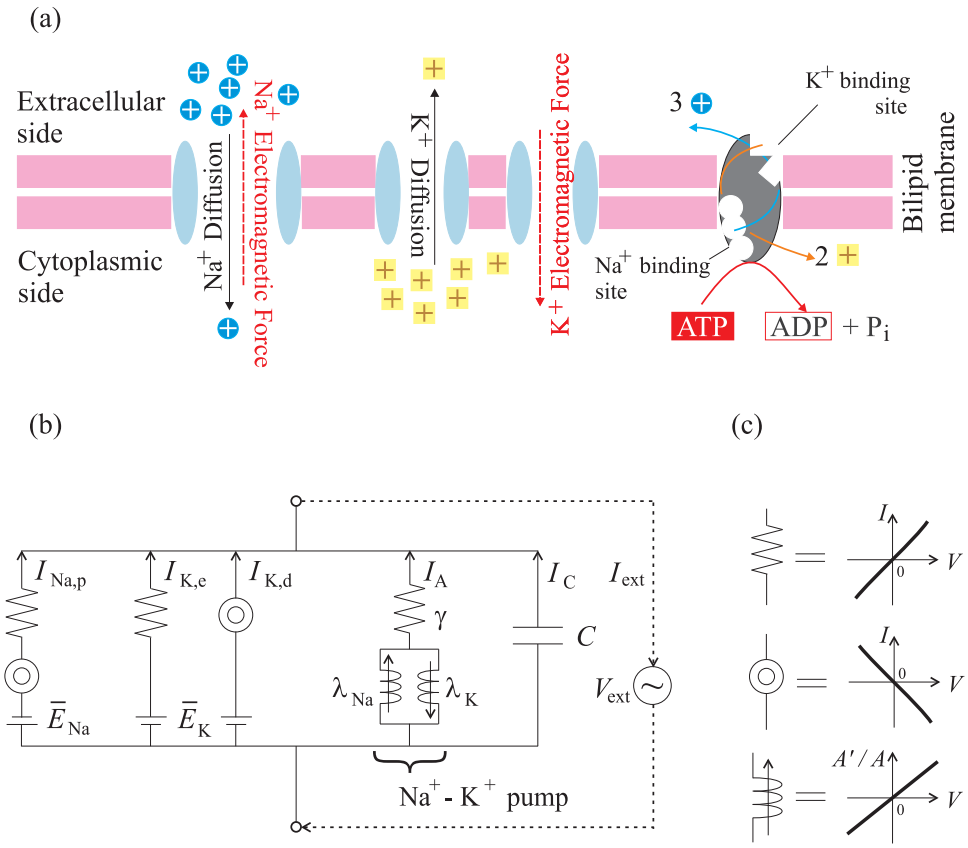

Figure 1: (a) A conceptual model of generic neurons with passive serial Na^+ channels, passive parallel K^+ channels, and an active Na^+-K^+ ion pump. (b) A circuit model of the conceptual neuron model. (c) The IV-characteristics of circuit elements modeling both the passive and the active channels.

allow any number of ion species with or without such duplications. For the most part of our exposition, however, we will use the sodium Na^+ ion and the potassium K^+ ion to illustrate the general methodology. Specifically, Fig.1 is an illustration for one type of the models that will be used as a prototypical example throughout the paper. Any inclusion from, say, Cl^- or Ca^{2+} will at least duplicate one element of such a minimal model. The Na^+-K^+ combination shown here can be substituted or modified by the inclusion of other ion species such as a Na^+-Ca^{2+} pair or a Na^+-K^+-Cl^- triplet as long as they are permitted by neurophysiology. This section is for the model construction and classification. Model analysis will be given in Sec.3.

2.1. The Conceptual Model. The conceptual model consists of a set of assumptions on passive and active channels. Passive channels are of two kinds: the *electro current* driven by the electromagnetic force from *all* charged ions; the *diffusive current* resulted from the concentration-induced transmembrane diffusion of a *particular* ion species. Neither of the two forces is facilitated by any conversion of biochemical energy of the cell. In contrast, an *active current* is due to the transmembrane transport of an ion species from an energy-converting, i.e., ATP-to-ADP (ATPase), ion pump, hence referred to as an active channel. The assumptions below are for some conceptual and

general properties of these channels, for which an illustration is given by Fig.1.

Circuit Model – Generic Assumptions:

(a) Each electro current I_e through a channel is characterized by a monotonically *increasing* function $I_e = \phi(V_e)$ of the voltage V_e across the channel. The channel or any device or structure whose current-voltage relation is characterized by such a monotonically increasing IV-characteristic curve is called a *conductor* (following a convention in neurophysiology although it is called a resistor in the general field of circuit).

(b) Each diffusive current I_d through a channel is characterized by a monotonically *non-increasing* function $I_d = \phi(V_d)$ of the voltage V_d across the channel. The channel or any device or structure whose current-voltage relation is characterized by a monotonically decreasing IV-characteristic curve is called a *diffusor*.

(c) Each active current through a channel has a fixed current direction and the time rate of change of the current is proportional to the product of the current and the voltage across the channel. The channel or device or structure whose current-voltage relation satisfies this condition is called a *pump*.

(d) All ion channels are resistive to electromagnetic force, large or small.

(e) Unless assumed otherwise, all active and passive currents between different ion species are in parallel across the cell membrane.

(f) The impermeable bilipid cell membrane is modeled as a capacitor.

We note that by the term channel it can mean the whole, or a constitutive part, or just an intrinsic property of a biophysical structure such as a voltage or protein mediated ion gate. Hypothesis (a) is the standard Ohm's law, but it can be considered to model the opening and closing of an ion species' voltage gate — the higher the voltage, the more openings of the gate, and the greater the electro current from all ions. It is probably a less mechanistic but definitely a more circuit-direct approach than that of Hodgkin-Huxley's by which the opening probability of the gate is modeled as a voltage-gated time evolution. Hypothesis (b) is justified by invoking the diffusion principle that atoms have the propensity to move against their concentration gradient. For ions the electrical effect of the diffusion is exactly opposite the electromagnetic force: A net extracellular concentration of a cation (positive charged ion) generates an higher electromagnetic potential on the outside, giving rise to an outward direction for the electro current. But the higher external concentration of the cation generates a diffusion-induced inward current, giving rise to the non-increasing IV-characteristic of a diffusor, see Fig.1(c). Again, a particular IV-curve would be a phenomenological fit to the analogous opening and closing of the diffusive type of ion gates which is modeled differently by HH type models in terms of gate opening probabilities. Note that because voltage potential can be set against an arbitrary basal constant, we can require without

loss of generality that the IV-curves for both conductors and diffusors to go through the origin for simplicity and definitiveness:

$$\phi(0) = 0.$$

However, a particular passive channel may have a non-zero resting potential, $\bar{E}$, which is modeled as a battery for voltage source, and the combined IV-characteristic curves will differ only by an $\bar{E}$-amount translation along the voltage variable. (More specific descriptions later.)

Hypothesis (c) is less immediately apparent, but can be justified at least conceptually as follows. Unlike passive ion channels, which have topologically straightforward pathways in most cases, ion pumps have a more involved and convoluted geometry [22]. In particular, we can assume that the ions wind through the pump in a helical path [14, 18]. In other words, the energy exchange between ATP and the pump sends the ions through a spiral path much like electrons moving through a coiled wire. However, unlike a coiled wire inductor, individual ion current has a fixed direction with Na^+ going out and K^+ going in. The simplest functional form for an ion pump that captures both its inductor-like feature and its one-way directionality is the following

$$A' = \lambda A V \tag{1}$$

where V is the voltage across the pump, A is the particular ion's active current through the pump, and λ is referred to as the *pump coefficient*, see Fig.1(c). Proportionality between the derivative of the current and the voltage models the pump as an inductor. Proportionality between A' and A preserves the directionality of A, that is, $A(0) > 0$ if and only if $A(t) > 0$ for all t. In addition, the smaller $A(t)$ is, the fewer ions are available there for transportation, and hence the smaller the rate of current change, $A'(t)$, in magnitude becomes. In other words, this model of ion pumps can be considered as a nonlinear inductor mediated by its own current for fixed directionality and strength. (For a more elaborative approach, one can replace the linear factor A by a functional with saturation, such as a Monod function $\frac{A}{1+bA}$ or some variants of it.)

Hypothesis (d) is certainly true wherever electromagnetic field is present. A passive conductor automatically takes it into consideration. A passive diffusor does not have to have this because its IV-curve can be assumed to have already absorbed such a resistance implicitly. For the Na^+-K^+ ion pump, we only need to wire such a parasitic resistor in series to fulfill this hypothesis, see Fig.1(b). The resistance, $\gamma > 0$, will be assumed small for the paper. Hypotheses (e) is a provisional assumption for this paper. It can be modified to allow different ions to go through a same physical channel, see remarks on Hypothesis (2) of the specific $pK^+_-sNa^+_+$ and $pNa^+_+sK^+_-$ models below. Hypotheses (f) is a standard assumption on electrophysiology of neurons.

2.2. Circuit Symbols and Terminology. For this paper, we will take the outward direction as the default current direction for all passive channels. One exception to this convention is for active currents whose directions are fixed and thus whose fixed directions are taken to be the default and the true directions, see Fig.1(b). Another exception is for the external current (such as synaptic currents or experimental controls with or without voltage clamp), I_{ext}, whose default direction is

chosen inward to the cell. We will use standard circuit symbols wherever apply and follow them closely when introducing new ones.

Mimicking the contour plot for mass concentration, the concentric-circle symbol, see Fig.1(b,c), is used for diffusors. In circuitry, a device having a decreasing IV-characteristics is called a negative resistor. In practice, it usually comes with both positive and negative resistive regions, such as the combined conductors and diffusors in series and parallel as illustrated in Fig.2. Electrical devices with a purely decreasing IV-curve are not usually encountered in practice and hence have not acquired a symbol in the literature. We use it here only to emphasize and to contrast the role of transmembrane diffusion of ions in comparison to their electromagnetic effect.

The conventional symbol for a nonlinear resistor with a non-monotonic IV-curve such as an S-shaped or N-shaped curve consists of a slanted arrow over a linear resistor symbol. We will not use it here for our conductor-diffusor combinations in series or in parallel because it has been used exclusively for the HH type circuit models of neurons that combines both the passive and *the active* currents as one conductance-based channel. For this main reason, the serial aggregation and the parallel aggregation each acquires a slightly modified symbol to the European symbol of resistors, shown in Figs.2, 3. The symbol for a *serial conductor-diffusor* is a vertical box circumscribing a letter S because the serial connectivity always results in an IV-curve with V as a function of I, $V = h(I)$, by Kirchhoff's Voltage Law, and usually in the shape of a letter S when it becomes non-monotonic. Similarly, the symbol for a *parallel conductor-diffusor* is a horizontal box circumscribing a letter N because the parallel connectivity always results in an IV-curve with I as a function of V, $I = f(V)$, by Kirchhoff's Current Law, and usually in the shape of a letter N when it becomes non-monotonic. We note that the IV-characteristic of a serial conductor-diffusor and a parallel conductor-diffusor when both are again connected in parallel can be monotonic or non-monotonic, a function of V or a function of I or neither, but most likely a curve implicitly defined by an equation $F(V, I) = 0$. As a result, it is represented by a square circumscribing a diamond symbolizing the typical fact that it may not be a function of V or I.

As mentioned earlier that once a common reference potential is set, a given ion's passive channel can have a *passive* resting potential, denoted by $\bar{E}_{\rm J}$ for ion J, which is defined by the equation $F(\bar{E}_{\rm J}, 0) = 0$ if the equation $F(V, I) = 0$ defines the complete IV-characteristic, whether or not it defines a function of V, or I, or neither. However, when all ion species other than ion J are blocked to cross the cell membrane, the dynamics of ion J may settle down to an equilibrium state. By definition, the equilibrium state's membrane potential component is called the *membrane* resting potential or the *active* resting potential, denoted by $E_{\rm J}$, if the corresponding active (pump) current $A_{\rm J} > 0$ is not zero. We will see later that the passive resting potential, $\bar{E}_{\rm J}$, can be alternatively defined to correspond to an equilibrium state at which $A_{\rm J} = 0$.

The symbol for ion pumps is similar to inductors because of their functional similarity but with an arrow for their one-way directionality. A standard linear inductor symbol with a slanted arrow stands for a variable inductor.

Recall that the IV-curve for a conductor is increasing or nondecreasing and the IV-curve for

a diffusor is decreasing or non-increasing. However, this is a rather imprecise definition. Without further constraint, even a linear conductor $I = gV$ can be artificially decomposed into a conductor and a diffusor in parallel:

$$gV = (g - d)V + dV$$

for any $d < 0$. Thus, to avoid such arbitrary cancellations between conductors and diffusors of equal strength, we will follow a normalizing rule to decompose an IV-curve into either a *linear* conductor, or a *linear* conductor and a *nonlinear* diffusor with zero maximal diffusion coefficient. This form of decomposition is called *canonical*.

More precisely, let $I = f(V)$ be an IV-characteristic which we want to decompose into a canonical form in parallel. Let $g = \max\{\max_V f'(V),\ 0\} \geq 0$ (with the maximum taken perhaps over some finite effective range). Then we have by Kirchhoff's Current Law,

$$I = f(V) = gV + [f(V) - gV] := f_{\rm e}(V) + f_{\rm d}(V),$$

for which $f_{\rm d}(V) = f(V) - gV$ is non-increasing since its maximal diffusion coefficient is given by $\max f_{\rm d}{}'(V) = \max(f'(V) - g) = 0$, showing the decomposition is canonical. (Here by definition, the rate of change $f'(V)$ is the *diffusion coefficient* if $f'(V) \leq 0$ and the *conductance* if $f'(V) \geq 0$.) We can further write the diffusor IV-curve as

$$[f(V) - gV] = d\frac{f(V) - gV}{d},\ \text{ if }\ d = \min\{\min_V[f'(V) - g],\ 0\} \leq 0,$$

with d being the maximal diffusion coefficient in magnitude. Similarly, if $V = h(I)$ is the IV-curve, then by Kirchhoff's Voltage Law, the canonical decomposition in series is

$$V = h(I) = \frac{1}{g}I + \frac{1}{d}[d(h(I) - \frac{1}{g}I)] := h_{\rm e}(I) + h_{\rm d}(I),$$

where $1/g = \max\{\max_I h'(I),\ 0\}$ and $1/d = \min\{\min_I[h'(I) - 1/g],\ 0\}$. Note that parameters g and d are the necessary minimum to determined a serial or parallel conductor-diffusor; and that the parallel (resp. serial) IV-curve is nondecreasing if and only if $g + d \geq 0$ (resp. $1/g + 1/d \geq 0$ or $g + d \leq 0$). As an illustration of the procedure, one can check that the canonical form for a linear conductor $I = gV$ is itself.

Note that the canonical decomposition has a symmetric form by exchanging the roles of conductors and diffusors: to decompose an IV-characteristic into either a *linear* diffusor, or a *linear* diffusor and a *nonlinear* conductor with zero minimal conductance. A given conductor-diffusor will be decomposed in one of the two forms but not necessarily in both forms as in the case that a linear conductor $V = gI$ can only have the canonical decomposition and a linear diffusor $V = dI$ can only have the opposite. However, we will explain later that the canonical decomposition is more probable for ions' passive channels than its symmetric counterpart because of the fact that the electromagnetic force governs all ions while a particular ion's diffusive current depends only on that particular ion's concentration gradient. Nevertheless, despite such differences in decomposition of a nonlinear IV-characteristic when both decompositions apply, all circuit properties

derived from the characteristic will remain the same because of the circuit equivalence guaranteed by Kirchhoff's Laws. Thus, unless stated otherwise, all IV-characteristic decompositions discussed from now on are canonical.

The cell membrane or a channel is said to *depolarize* if its voltage moves toward $V = 0$. If the voltage moves away from $V = 0$ the membrane or the channel is said to *hyperpolarize*. Thus, a negative increase or a positive decrease in a voltage is a depolarization of the voltage, and in contrast, a negative decrease or a positive increase is an hyperpolarization of the voltage.

2.3. Model Classification and Result Summary. We will adopt a notation convention for our neural models. Take for example, the model $\mathrm{pK}^+_-\mathrm{sNa}^+_+$ to be discussed below stands for the following. The lower case "p" before K^+ means that the passive channels of K^+'s are in *parallel* and that K^+'s diffusive channel can be dominating in some effective region of the dynamical states so that the combined IV-characteristic of the parallel conductor-diffusor is not monotonic in the region. Similarly, the lower case "s" means the same except that the passive channels of Na^+'s are in *series*. The subscript is used for ion pump information. In this case, for example, $\mathrm{pK}^+_-\mathrm{sNa}^+_+$ symbolizes the assumption that K^+ is pumped *into* the cell while Na^+ is pumped *outside* the cell by the Na^+-K^+ ion pump. On the other hand, a subscript "0" means the absence of an ion pump for its designated ion. So, model $\mathrm{pK}^+_0\mathrm{sNa}^+_+$ denotes the same $\mathrm{pK}^+_-\mathrm{sNa}^+_+$ model except for the assumption that the neuron does not have a K^+ ion pump. Also, we will use subscripts $-d, +d$, such as in $\mathrm{pK}^+_{-d}\mathrm{sNa}^+_{+d}$, to denote ion pumps not combined in structure but rather operating independently on their own. A circuit diagram for such models, slightly different from Fig.1 in the ion pump structure, will be given near the end of the paper.

As it will be shown later, the direction of an ion pump will fix the polarity of the ion's passive resting potential *if* the ion species' active resting potential exists. More specifically, if Na^+ (resp. K^+) has an active (membrane) resting potential (which is usually the case), then the assumption that Na^+ (resp. K^+) is pumped outward (resp. inward) implies $\bar{E}_{\mathrm{Na}} > E_{\mathrm{Na}} > 0$ (resp. $\bar{E}_{\mathrm{K}} < E_{\mathrm{K}} < 0$). That is, the polarities of both passive and active resting potentials are fixed to be the same by the directionalities of the ion pumps.

This basic scheme can be extended in a few ways. In one extension, for example, if both passive and active channels of the Na^+ ion are blocked, the reduced system can be considered as a pK^+_- model. In another extension, for example, if in the effective region of the neuron's dynamical states, Na^+'s diffusion does not dominate but its ion pump is nonetheless effective, we can use $\mathrm{pK}^+_-\mathrm{cNa}^+_+$ to denote the model in that part of the effective region, with the lower case "c" for the *conductive* nature (i.e. monotonically increasing) of that part of its IV-characteristic. Furthermore, the notation for the corresponding serial conductor-diffusor can be reduced to a vertical box with a diagonal line from the lower-left corner to the upper-right corner rather than a circumscribed letter "S". Similar notation and symbol can be extended to parallel conductor-diffusors without diffusion domination. In another extension, more ion species can be included. For example, all our simulations of this paper were actually done for a $\mathrm{pK}^+_-\mathrm{sNa}^+_+\mathrm{cCl}^-_0$ (with $g_{\mathrm{Cl}} = 0.01,\ d_{\mathrm{Cl}} = 0,\ \bar{E}_{\mathrm{Cl}} = -0.6$), which, to become apparent later, is equivalent to a minimal $\mathrm{pK}^+_-\mathrm{sNa}^+_+$ model.

Table 1: Dynamical Features

Models	Resting Potentials	Action Potentials	Spike-Bursts
cX	✓	x	x
sX	✓	–	x
sXcY	✓	–	x
pX	✓	✓	x
pXcY	✓	✓	x
pXsY	✓	✓	✓

We remark that a $pK^+_-pNa^+_+$ or $cK^+_-pNa^+_+$ model may fit well to the giant squid axon, but not all models from the taxonomy can necessarily find their neurophysiological counterparts. Also, it will become clear later that from the viewpoint of equivalent circuit, a $pK^+_-cNa^+_0$ model is usually equivalent to a pK^+_- model, but a $pK^+_-cNa^+_+$ or $pK^+_-sNa^+_0$ model may not be so in general because of the ion pump inclusion for the former and a possible S-nonlinearity of the Na^+ion for the latter. In addition, the taxonomy is order independent: xXyY and yYxX denotes the same model.

There will be three types of neural dynamics considered: resting membrane potentials, membrane action potentials (pulses or spikes), and spike-bursts. Resting potentials are stable equilibrium states in some membrane potential and current ranges where diffusion does not dominate from any ion species. In other words, stable equilibrium states are prominent features of cX models. On the other hand, action potentials and spike-bursts are oscillatory states and their generations require diffusion domination of some ion species in some finite range of the effective range of the oscillations. More specifically, action potentials require diffusion domination from only one ion species over its parallel conductive channel while spike-bursts require diffusion domination from at least two ion species, one over its parallel conductive channel and another over its serial conductive channel. Hence, for the purpose of distinction, a K^+-*mediated action potential* is the result of K^+'s diffusion domination in parallel, while a Na^+-mediated action potential is the result of Na^+'s diffusion domination in parallel. That is, action potentials is the prominent features of pX and pXcY models. Similarly, a Na^+-K^+ *spike-burst* is the result of a K^+-mediated burst of Na^+-mediated spikes because of K^+'s diffusion domination in parallel for the burst and Na^+'s diffusion domination in series for the spikes, respectively, the prominent feature of a $pK^+_-sNa^+_+$ model. Similar description applies to K^+-Na^+ spike-bursts for a $pNa^+_+sK^+_-$ model. We note that an xX model is a subsystem of an xXyY model and as a result the prominent dynamical behavior of the xX system will be a feature, though not prominent one, of the larger xXyY system. Thus, one should expect resting potential state, action potential phenomenon in a pXyY model. A summary of the result is listed in Table 1, in which a "–" entry means "possible but unlikely".

All numerical simulations will be done in this paper for dimensionless models because of two reasons. One, numerical simulations tend to be more reliable when all variables and parameters are restricted to a modest, dimensionless range. Two, the dimensionless models can always be

changed to dimensional ones by scaling the variables and parameters accordingly.

2.4. Specific Models. We will consider several specific models in the paper, all based two specific models introduced here in this section: the $\text{pK}^+_-\text{sNa}^+_+$ model and the $\text{pNa}^+_+\text{sK}^+_-$ model, respectively. Their specific channel structures are illustrated in Fig.2(a,b) and Fig.2(c,d), respectively. We now introduce them in detail one at a time.

The $\text{pK}^+_-\text{sNa}^+_+$ Model:

1. K^+'s conductive and diffusive currents go through separate parallel channels for which an increase (hyperpolarization) in a positive voltage range, $0 < v_1 < v_2$, of the diffusor triggers a negative drop (inward flow) of its current, see Fig.2(a).
2. Na^+'s conductive and diffusive currents go through the same channel for which an increase in an outward (positive) current range, $0 < i_1 < i_2$, of the diffusor triggers a negative hyperpolarization (decrease) in the voltage, see Fig.2(b).
3. Both ion species have an active resting potential each, satisfying $E_{\text{Na}} > 0$ and $E_{\text{K}} < 0$.
4. There is an ion pump for each ion species with the active Na^+ current, A_{Na}, going inward and the active K^+ current, A_{K}, going outward. Both share a common structure in the sense that they have the same pump parameter values: $\lambda_{_{\text{K}}} = \lambda_{_{\text{Na}}} = \lambda$ and a small resistance $\gamma > 0$.

These hypotheses are formulated mainly from a minimalistic principle. This includes: (i) the ion species do not duplicate each others functions; (ii) a diffusor is included only if it can fundamental change the combined IV-characteristic to a non-monotonic curve; (iii) the S-shaped and the N-shaped IV-characteristics overlap in an effective or common voltage region; and (iv) the polarities, $E_{\text{Na}} > 0$ and $E_{\text{K}} < 0$, for the active resting potentials are fixed, which are approximately in the ranges of ~ 80 mV and ~ -90 mV, respectively. All alternative configurations that we have checked have violated at least one of the four minimalistic criteria for the $\text{pK}^+_-\text{sNa}^+_+$ model above. More detailed comments on the hypotheses follow below.

By Hypothesis 1 and Kirchhoff's Current Law, the passive K^+ current $I_{\text{K,p}}$ is the sum of its conductor current, $I_{\text{K,e}}$, and its diffusor current, $I_{\text{K,d}}$, with the same passive voltage V_{K} across the conductor and the diffusor in parallel. Thus, the IV-characteristic curve for the parallel K^+ conductor-diffusor (Fig.2(a)) is

$$I_{\text{K,p}} = I_{\text{K,e}} + I_{\text{K,d}} = f_{\text{K,e}}(V_{\text{K}}) + f_{\text{K,d}}(V_{\text{K}}) := f_{\text{K}}(V_{\text{K}}) \tag{2}$$

where functions $f_{\text{K,e}}$ and $f_{\text{K,d}}$ define the individual monontone IV-curves for the conductor and diffusor, respectively. After adjusted for the passive resting potential (battery source) $\bar{E}_{\text{K}} = V_{\text{C}} - V_{\text{K}}$, we have,

$$I_{\text{K,p}} = f_{\text{K}}(V_{\text{C}} - \bar{E}_{\text{K}}). \tag{3}$$

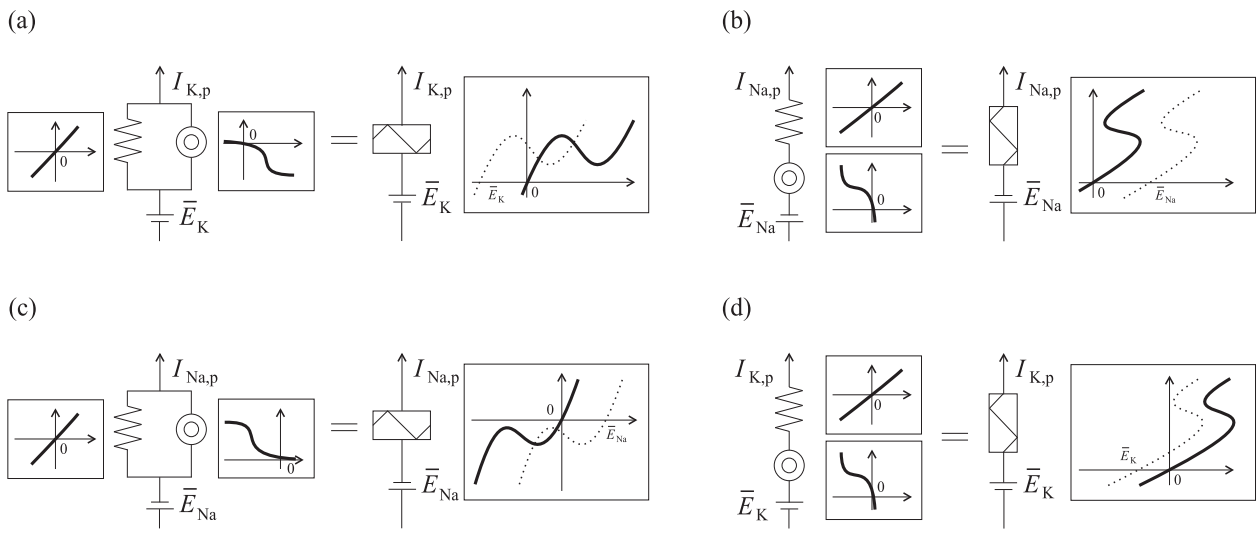

Figure 2: The $\text{pK}^{+}_{-}\text{sNa}^{+}_{+}$ model: (a) An N-shaped IV-curve (solid) for a parallel conductor-diffusor of the passive K^+'s channels. It is the vertical sum of the conductor and diffusor curves. (b) An S-shaped IV-curve (solid) for a serial conductor-diffusor of the passive Na^+'s channels. It is the horizontal sum of the conductor and diffusor curves. Dash curves are the solid curves' horizontal translations to their respective nonzero passive resting potentials, giving rise to the final IV-curves for the respective passive channels. (c, d) The same description but for the $\text{pNa}^{+}_{+}\text{sK}^{+}_{-}$ model. Both models retain the same polarities for the passive resting potentials, $\bar{E}_{\text{Na}} > 0, \bar{E}_{\text{K}} < 0$.

Throughout most of the paper, we will consider an N-shaped nonlinearity as shown in Fig.2(a), which is the result of the diffusion domination of K^+ in the range $[v_2 + \bar{E}_{\text{K}}, v_2 + \bar{E}_{\text{K}}]$. This hypothesis can be interpreted like this. When the membrane potential lies in this range, it is mainly due to a correspondingly uneven distribution of K^+ across the cell wall, which in turn triggers the diffusion-driven flow of the ion. However, when the membrane potential lies outside the range, its characteristic is mainly due to factors other than K^+'s uneven distribution across the membrane.

More specifically, all conductor-diffusor decompositions of Fig.2 are canonical. A justification of this choice is based on a key distinction between the electro force and the diffusive force. The former is defined by all ion species, while the latter is defined only by a particular ion which is a constituent part of the former. Because of a fixed amount of that given ion species, its diffusive effect occupies only a subrange of the whole electro range. This gives a conceptual justification for the ramp-like functional form for the diffusor characteristic. That is, outside the ramping voltage range, a given ion's biased concentration on one side of the cell wall approaches an all-or-nothing saturation, inducing an approximately constant diffusive current flux through the membrane. Within the ramping range, however, the diffusive current is more or less in proportion to the membrane potential. Again, the requirement $\phi(0) = 0$ for the characteristics is set against some basal references collected into the passive resting potential parameters $\bar{E}_{\text{J}}$.

It will become clear later that action potential depolarization from rest cannot be easily generated without the N-nonlinearity. The left and right branches of an N-curve have positive slopes,

corresponding to the voltage region where the conductive current dominates the diffusive current. They are referred to as the *conductive branches* or the *conductor dominating branches*. Although it is possible for both branches to intersect the V-axis in a so-called bistable configuration, we will consider for most of the exposition the case of a unique intersection by only one of the two branches, for which the branch that intersects the V-axis is called the *primary branch*. We will see later that the intersection is the passive resting potential $\bar{E}_{\rm K}$. The middle branch is called the *diffusive branch* or the *diffusor dominating branch*.

By Hypothesis 2 and Kirchhoff's Voltage Law, the passive Na^+ voltage $V_{\rm Na}$ is the sum of its conductive voltage, $V_{\rm Na,e}$, and its diffusive voltage, $V_{\rm Na,d}$, with the same passive Na^+ current $I_{\rm Na,p}$ going through the conductor and the diffusor in series. The IV-characteristic curve for the serial Na^+ conductor-diffusor (Fig.2(b)) is

$$V_{\rm Na} = V_{\rm Na,e} + V_{\rm Na,d} = h_{\rm Na,e}(I_{\rm Na,p}) + h_{\rm Na,d}(I_{\rm Na,p}) := h_{\rm Na}(I_{\rm Na,p}), \tag{4}$$

where functions $h_{\rm Na,e}$ and $h_{\rm Na,d}$ define the individual monotonic IV-curves for the conductor and diffusor, respectively. After adjusted for the passive resting potential (battery source) $\bar{E}_{\rm Na}$, we have

$$V_{\rm C} = V_{\rm Na} + \bar{E}_{\rm Na} = h_{\rm Na}(I_{\rm Na,p}) + \bar{E}_{\rm Na}. \tag{5}$$

Throughout most of the paper, we will consider an S-shaped nonlinearity as shown in Fig.2(b). Again, a similar interpretation can be made for the diffusion domination of Na^+ in the current range $[i_1, i_2]$ as that of K^+ in the voltage range $[v_1 + \bar{E}_{\rm K}, v_2 + \bar{E}_{\rm K}]$ from Hypothesis 1.

It turns out from our analysis of our minimalistic models that the models will not produce a spike-burst phenomenon without an S-shaped IV-characteristic of one ion species or some combination of different ion species. One the other hand, an S-shaped characteristic can only be generated from a conductor and a diffusor in series, but not in parallel. Therefore, it is the spike-burst phenomenon and the circuit imperative that imply the serial structure of a conductive current and a diffusive current. It is not important whether the conductive current and the diffusive current are from a single ion species or from different ion species to share a same physical channel. It matters only that the serial combination produces such an S-shaped characteristic. However, in the case that a different ion species (such as K^+, or Ca^{2+}, or Cl^-, or a combination thereof) is involved, this hypothesis can be generalized to have Na^+'s *conductive* current and that other ion's *diffusive* current, in part or whole, to go through the same channel, and the same results to be obtained will remain true. In other words, assuming the serial channel sharing for Na^+ of this model and for K^+ of the next model is simply a sufficient way to guarantee such a necessary condition for spike-bursts. As we will show later that this hypothesis is not needed for the existence of resting potentials, passive or active, nor for the generation of action potentials.

Similar terminology applies to the S-nonlinearity. Specifically, the top and bottom parts have positive slopes, resulted from the conductor's dominating IV-characteristic in the respective current ranges. They are referred to as the *conductive* or *conductor dominating branches*. Of the two branches, the branch that intersects the V-axis is referred to as the *primary* branch or the primary

conductive branch. Again we will see later that the intersection is the passive resting potential $\bar{E}_{\rm Na}$. In contrast, the middle branch with negative slopes is referred to as the *diffusive branch* or the *diffusor dominating branch*.

Hypothesis 3 was already commented above. Hypothesis 4 is a well-known property of most neurons. We note that although there is a frequently-cited 3:2 stoichiometric exchange ratio for the Na^+-K^+ ATPase, we do not tie the active currents $A_{\rm Na}, A_{\rm K}$ to the same ratio, especially not at a non-equilibrium state of the membrane potential. The exchanger certainly has an optimal exchange ratio for each ATPase, but it does not have to operate at its optimal capability all the time because one can envision a situation in which a severely depleted extracellular concentration of K^+ just cannot meet the maximal demand of 2 potassium ions for every exchange. The same argument applies to Na^+. This non-constant-exchange hypothesis for Na^+-K^+ ATPase is also the basis to segregate the net ion pump current $I_{\rm A}$ into the $A_{\rm Na}$ and $A_{\rm K}$ currents:

$$I_{\rm A} = A_{\rm Na} - A_{\rm K}.$$

Exchanging the roles of Na^+ and K^+ in the $pK^+_-sNa^+_+$ model with a few modifications results in the $pNa^+_+sK^+_-$ model below. More specifically, we have

The $pNa^+_+sK^+_-$ Model:

(1) Na^+'s electro and diffusive currents go through separate parallel channels for which a depolarization (increase) in a negative voltage range, $v_1 < v_2 < 0$, of the diffusor triggers a positive drop in its outward (positive) current, see Fig.2(c).

(2) K^+'s electro and diffusive currents go through the same channel for which an increase in an outward (positive) current range, $0 < i_1 < i_2$, of the diffusor triggers a negative hyperpolarization (decrease) in its voltage, see Fig.2(d).

(3) Both ion species have an active resting potential each, satisfying $E_{\rm Na} > 0$ and $E_{\rm K} < 0$.

(4) There is an ion pump for each ion species with the active Na^+ current, $A_{\rm Na}$, going inward and the active K^+ current, $A_{\rm K}$, going outward. Both share a common structure in the sense that they have the same pump parameter values: $\lambda_{_{\rm K}} = \lambda_{_{\rm Na}} = \lambda$ and a small resistance $\gamma > 0$.

In addition to the role reversal, there is a marked difference between these two models for Hypothesis (1) in the diffusor-dominating voltage range: for the $pK^+_-sNa^+_+$ model, the range satisfies $0 < v_1 < v_2$ whereas for the $pNa^+_+sK^+_-$ model, the range satisfies $v_1 < v_2 < 0$, see Fig.2(a,c). This specific range assumption for each model is based on the minimalistic criterion (iii) so that the model's S-characteristic and the N-characteristic can affect each other in a common and close proximity possible. Hypothesis (2) remains the same from the previous model except for the role exchange between the ions. On the other hand, Hypotheses (3,4) are identical for both models,

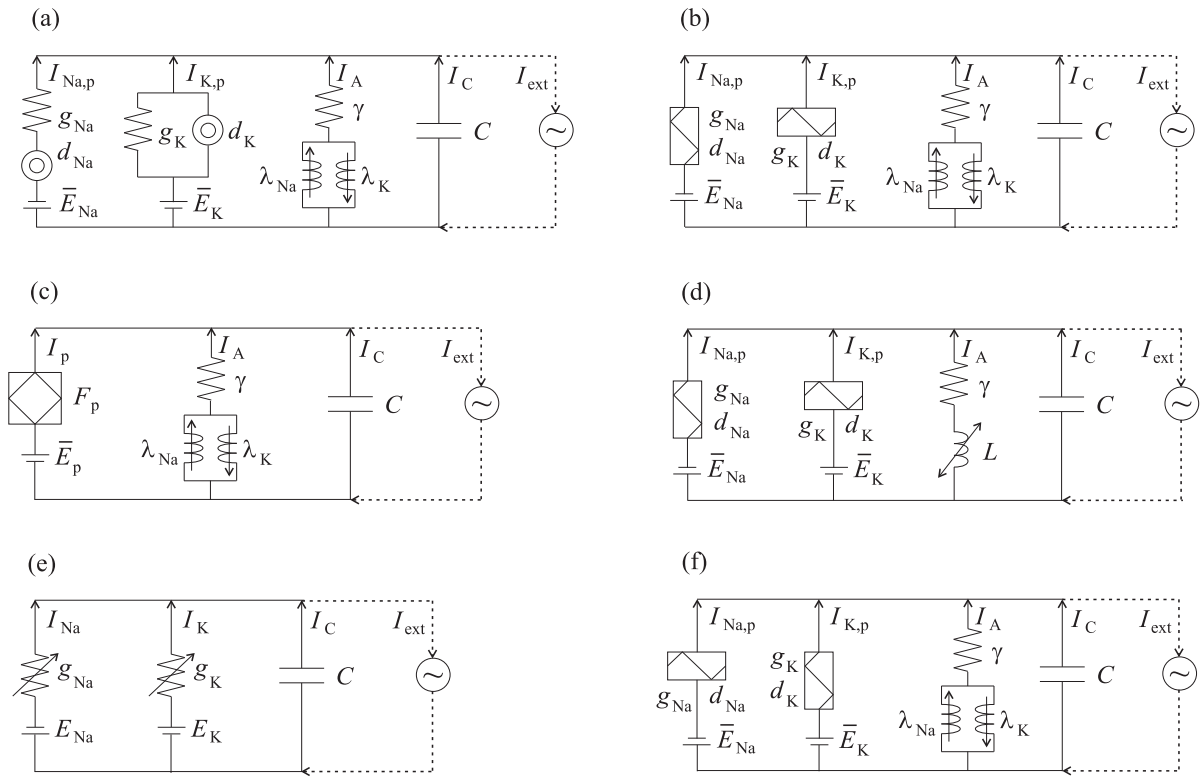

Figure 3: Equivalent Circuits.

which are listed here for the completeness of the second model. Because of the symmetrical similarities between the $\mathrm{pK}^{+}_{-}\mathrm{sNa}^{+}_{+}$ model and the $\mathrm{pNa}^{+}_{+}\mathrm{sK}^{+}_{-}$ model, detailed analysis from now on will be given mainly to the $\mathrm{pK}^{+}_{-}\mathrm{sNa}^{+}_{+}$ model. Note also, the depiction of neuromembrane of Fig.1 is in fact for the $\mathrm{pK}^{+}_{-}\mathrm{sNa}^{+}_{+}$ model.

2.5. Equivalent Circuits. There are different but equivalent ways to represent the circuit model Fig.1(b) depending on how individual channels are selectively grouped. The ones that will be used and discussed in this paper are illustrated in Fig.3 for the $\mathrm{pK}^{+}_{-}\mathrm{sNa}^{+}_{+}$ model, but we remark that the main equivalent circuit to be used for the analysis and simulation of the paper is that of Fig.3(b). Except for Fig.3(f), not all analogous circuits for the $\mathrm{pNa}^{+}_{+}\mathrm{sK}^{+}_{-}$ model are shown since they can be derived similarly.

More specifically, Fig.3(a) is the same circuit as Fig.1(b) except that the passive electro and diffusive K^{+} channels are grouped together and the optional external inward current or voltage source is redrawn simply as another parallel channel.

Fig.3(b) is the same as (a) except that both ions' passive channels are represented by a combined conductor-diffusor in series (Eq.(5)) and a combined conductor-diffusor in parallel (Eq.(3)), respectively. And for most of the analysis and discussion, we will assume the S-nonlinearity and the N-nonlinearity of Fig.2 for Na^{+}'s IV-curve and K^{+}'s IV-curve, respectively.

Circuit Fig.3(c) is the same circuit as (b) except that all passive channels are combined into one super passive channel whose IV-curve is defined by an equation $F_{\mathrm{p}}(V_{\mathrm{p}}, I_{\mathrm{p}}) = 0$ of Eq.(7). There

is no conceptual nor practical difficulty to construct such compositorial IV-curves *geometrically* based Kirchhoff's Voltage Law, see [2]. However, it seems not very practical to have a general algorithm for the defining equations of the IV-curves of such equivalent conductors and diffusors in arbitrary numbers. For example, it is rather straightforward to do so for the parallel combination of one serial-conductor-diffusor and one parallel-conductor-diffusor, which is the case here. Specifically, by Kirchhoff's Current Law, $I_{\rm p} = I_{\rm Na,p} + I_{\rm K,p}$. Also from $I_{\rm K,p} = f_K(V_{\rm C} - \bar{E}_{\rm K})$ we first have

$$I_{\rm Na,p} = I_{\rm p} - I_{\rm K,p} = I_{\rm p} - f_{\rm K}(V_{\rm C} - \bar{E}_{\rm K}).$$

Second, since $V_{\rm C} - \bar{E}_{\rm Na} = V_{\rm Na} = h_{\rm Na}(I_{\rm Na,p})$, we have

$$V_{\rm C} - \bar{E}_{\rm Na} = h_{\rm Na}(I_{\rm p} - f_{\rm K}(V_{\rm C} - \bar{E}_{\rm K})).$$

Rearrange this relation to have

$$F(V_{\rm C}, I_{\rm p}) := V_{\rm C} - \bar{E}_{\rm Na} - h_{\rm Na}(I_{\rm p} - f_{\rm K}(V_{\rm C} - \bar{E}_{\rm K})) = 0.$$

This equation does not necessarily satisfy $F(0,0) = 0$. As a result, we define the *passive resting potential*, $\bar{E}_{\rm p}$, to be the solution of

$$F(\bar{E}_{\rm p}, 0) = 0. \tag{6}$$

Finally, because $V_{\rm C} = V_{\rm p} + \bar{E}_{\rm p}$ we have the IV-curve's defining equation

$$F_{\rm p}(V_{\rm p}, I_{\rm p}) := F(V_{\rm p} + \bar{E}_{\rm p}, I_{\rm p}) = V_{\rm p} + \bar{E}_{\rm p} - \bar{E}_{\rm Na} - h_{\rm Na}(I_{\rm p} - f_{\rm K}(V_{\rm p} + \bar{E}_{\rm p} - \bar{E}_{\rm K})) = 0. \tag{7}$$

For the mathematical analysis to be carried out later, however, we will not use this equivalent form because it is more convenient to use individual ions' IV-curves in their segregated forms as for the cases of Figs.3(b,d). (But, a comparison simulation for a consistency check is given in Fig.10.)

Circuit Fig.3(d) is the same as Fig.3(b) except that the ion pump currents are combined into one active current according to the following relation:

$$\left\{ \begin{array}{l} I_{\rm A} = A_{\rm Na} - A_{\rm K} \\ I_{\rm S} = A_{\rm Na} + A_{\rm K} \end{array} \right. \text{ equivalently } \left\{ \begin{array}{l} A_{\rm Na} = \frac{1}{2}(I_{\rm S} + I_{\rm A}) \\ A_{\rm K} = \frac{1}{2}(I_{\rm S} - I_{\rm A}) \end{array} \right. \tag{8}$$

where $I_{\rm A}$ is the net active current through the ion pump and $I_{\rm S}$ is the sum of absolute currents exchanged by the ion pump. Let $V_{\rm A}$ be the voltage across the pump corresponding to the outward net current $I_{\rm A}$. Since $\gamma I_{\rm A}$ is the voltage across the resistive component of the pump and by Kirchhoff's Voltage Law, $V_{\rm C} = V_{\rm A} + \gamma I_{\rm A}$. Now from the IV-characteristic of the ion pump Eq.(1), we have

$$\left\{ \begin{array}{l} {A_{\rm Na}}' = \lambda_{\rm Na} A_{\rm Na} V_{\rm A} = \lambda A_{\rm Na}[V_{\rm C} - \gamma I_{\rm A}] = \lambda A_{\rm Na}[V_{\rm C} - \gamma(A_{\rm Na} - A_{\rm K})] \\ {A_{\rm K}}' = \lambda_{\rm K} A_{\rm K}[-V_{\rm A}] = \lambda A_{\rm K}[-V_{\rm C} + \gamma I_{\rm A}] = \lambda A_{\rm K}[-V_{\rm C} + \gamma(A_{\rm Na} - A_{\rm K})], \end{array} \right. \tag{9}$$

where $\lambda_{\rm Na} = \lambda_{\rm K} = \lambda$ by Hypothesis 4 of both models. The equivalent equations for $I_{\rm A}, I_{\rm S}$ are

$$\left\{ \begin{array}{l} {I_{\rm A}}' = \lambda I_{\rm S}[V_{\rm C} - \gamma I_{\rm A}] \\ {I_{\rm S}}' = \lambda I_{\rm A}[V_{\rm C} - \gamma I_{\rm A}]. \end{array} \right. \tag{10}$$

It is useful to note that we always have $I_{\rm S} > 0$ and that the nontrivial part ($I_{\rm A} \neq 0$) of $I_{\rm S}$'s nullcline is exactly the same as $I_{\rm A}$'s nullcline, $V_{\rm C} = \gamma I_{\rm A}$. Furthermore, the equation for $I_{\rm S}$ is rather simple and it can be solved explicitly in terms of the net current $I_{\rm A}$ as

$$I_{\rm S}(t) = I_{\rm S}(0) + \int_0^t \lambda I_{\rm A}(\tau)[V_{\rm C}(\tau) - \gamma I_{\rm A}(\tau)]\, d\tau. \tag{11}$$

As a result, the net active current satisfies

$$I_{\rm A}{}' = \frac{1}{L(t)}[V_{\rm C} - \gamma I_{\rm A}], \;\; \text{with} \;\; L(t) = \frac{1}{\lambda[I_{\rm S}(0) + \int_0^t \lambda I_{\rm A}(\tau)[V_{\rm C}(\tau) - \gamma I_{\rm A}(\tau)]\, d\tau]}. \tag{12}$$

In other words, the parallel ion pumps from circuit Fig.3(b) are equivalent to a nonlinear inductor of Fig.3(d) with L being the nonlinear inductance defined above. For the remainder of the paper, we will use both circuit (b) and circuit (d) interchangeably depending on whichever is simpler for a particular piece of analysis or simulation.

Circuit Fig.3(e) is the same circuit as (a) except that all passive and active K^+ channels are combined into one K^+ channel, $I_{\rm K} = I_{\rm K,p} + A_{\rm K}$, and all passive and active Na^+ channels are combined into one Na^+ channel, $I_{\rm Na} = I_{\rm Na,p} + A_{\rm Na}$, as conventionally done for all HH type models. Here one uses instead the ions' active resting potentials, $E_{\rm Na}, E_{\rm K}$, as the battery source offsets for the congregated ion channels. The precise relationship between the active and passive resting potentials will be derived later. We will not explore any quantitative comparison between these two types of models further in this paper except to note that it is not clear how to extract from circuit (e) some of the properties to be derived in this paper.

Fig.3(f) is a circuit diagram for the $\text{pNa}^+_+\text{sK}^+_-$ model. It is exactly the same as (a) except that the passive Na^+ channel is a parallel conductor-diffusor while the passive K^+ channel is a serial conductor-diffusor.

Notice that the circuit diagram (b) and (f) each is in a one-to-one qualitative correspondence to the $\text{pK}^+_-\text{sNa}^+_+$ model and the $\text{pNa}^+_+\text{sK}^+_-$, respectively. In other words, a circuit diagram can be uniquely constructed qualitatively from a model taxon and vice versa.

2.6. Equivalent Circuits in Differential Equations. We now cast the circuits in terms of their differential equations for simulation and analysis later. Because of the equivalence, a neuron model can be qualitatively described by its model taxon, or its circuit diagram, or its system of differential equations, with progressively greater details in description.

To begin with, all circuit models follow Kirchhoff's Current Law for all transmembrane currents:

$$I_{\rm C} + I_{\rm Na,p} + I_{\rm K,p} + A_{\rm Na} - A_{\rm K} - I_{\rm ext} = 0,$$

for which, as noted earlier, the directions of the active currents are fixed, and $I_{\rm ext}$ is directed intracellularly. With the capacitor relation

$$CV_{\rm C}{}'(t) = I_{\rm C}$$

Table 2: Equivalent Differential Equations

Circuit Fig.3(c)	$\begin{cases} CV_{\rm C}{}' = -[I_{\rm p} + A_{\rm Na} - A_{\rm K} - I_{\rm ext}] \\ A_{\rm Na}{}' = \lambda A_{\rm Na}[V_{\rm C} - \gamma(A_{\rm Na} - A_{\rm K})] \\ A_{\rm K}{}' = \lambda A_{\rm K}[-V_{\rm C} + \gamma(A_{\rm Na} - A_{\rm K})] \\ \epsilon I_{\rm p}' = F_{\rm p}(V_{\rm C} - \bar{E}_{\rm P}, I_{\rm p}) = V_{\rm C} - \bar{E}_{\rm Na} - h_{\rm Na}(I_{\rm p} - f_{\rm K}(V_{\rm C} - \bar{E}_{\rm K})) \end{cases}$
Circuit Fig.3(d)	$\begin{cases} CV_{\rm C}{}' = -[I_{\rm Na,p} + f_{\rm K}(V_{\rm C} - \bar{E}_{\rm K}) + I_{\rm A} - I_{\rm ext}] \\ I_{\rm A}{}' = \frac{1}{L}[V_{\rm C} - \gamma I_{\rm A}] \\ \epsilon I_{\rm Na,p}{}' = V_{\rm C} - \bar{E}_{\rm Na} - h_{\rm Na}(I_{\rm Na,p}) \\ \quad \text{with } L > 0 \text{ defined by (12)} \end{cases}$
Circuit Fig.3(f) (The $\text{pNa}^{+}_{+}\text{sK}^{+}_{-}$ Model)	$\begin{cases} CV_{\rm C}{}' = -[f_{\rm Na}(V_{\rm C} - \bar{E}_{\rm Na}) + I_{\rm K,p} + I_{\rm A} - I_{\rm ext}] \\ I_{\rm A}{}' = \lambda I_{\rm S}[V_{\rm C} - \gamma I_{\rm A}] \\ I_{\rm S}{}' = \lambda I_{\rm A}[V_{\rm C} - \gamma I_{\rm A}] \\ \epsilon I_{\rm K,p}{}' = V_{\rm C} - \bar{E}_{\rm K} - h_{\rm K}(I_{\rm K,p}). \end{cases}$

where C is the membrane capacitance in a typical range of $C \sim 1\mu\text{F}/\text{cm}^2$, the first differential equation for all circuits is

$$CV_{\rm C}{}'(t) = -[I_{\rm Na,p} + I_{\rm K,p} + A_{\rm Na} - A_{\rm K} - I_{\rm ext}].$$

The K^+ passive current can be replaced by its IV-curve $I_{\rm K,p} = f_{\rm K}(V_{\rm C} - \bar{E}_{\rm K})$ from (3). But the Na^+ passive current cannot be solved from its non-invertible, S-shaped IV-curve (hysteresis), $V_{\rm C} - \bar{E}_{\rm Na} = h_{\rm Na}(I_{\rm Na,p})$. Since $V_{\rm C}$ is not redundantly defined by the Na^+ passive current, but rather the other way around, the IV-relationship

$$F_{\rm Na}(V_{\rm C} - \bar{E}_{\rm Na}, I_{\rm Na,p}) := V_{\rm C} - \bar{E}_{\rm Na} - h_{\rm Na}(I_{\rm Na,p}) = 0$$

defines an ideal voltage-gated relationship for the passive current $I_{\rm Na,p}$. A standard and practical way ([2]) to simulate and to approximate this ideal IV-curve is to replace the algebraic equation above by a singularly perturbed differential equation as below,

$$\epsilon I_{\rm Na,p}{}' = F_{\rm Na}(V_{\rm C} - \bar{E}_{\rm Na}, I_{\rm Na,p}),$$

where $0 < \epsilon \ll 1$ is a sufficiently small parameter. More specifically, the positive sign (or lack of it) in front of $F_{\rm Na}$ is chosen so that the conductor-dominating branches of the IV-curve, $V_{\rm C} - \bar{E}_{\rm Na} = h_{\rm Na}(I_{\rm Na,p})$, are attracting and the diffusor-dominating middle branch is repelling for this auxiliary differential equation. It is useful to note that the nullcline, or the $I_{\rm Na,p}$-nullcline, of this equation

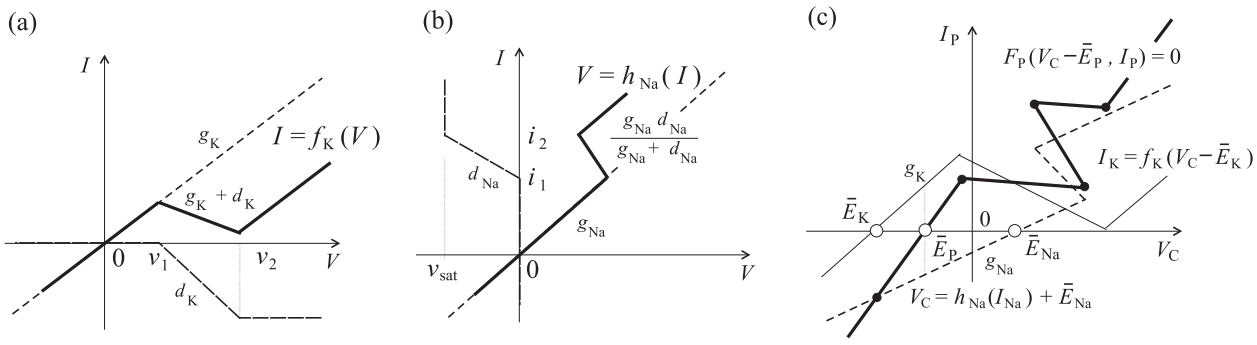

Figure 4: (a) Continuous and piecewise linear IV-curves for K^+'s parallel conductor-diffusor. The solid curve is the vertical sum of the dash curves. (b) Continuous and piecewise IV-curves for Na^+'s serial conductor-diffusor. The solid curve is the horizontal sum of the dash curves. (c) An equivalent IV-curve in bold solid when an S-shaped Na^+ conductor-diffusor IV-curve and an N-shaped K^+ conductor-diffusor IV-cure are combined in parallel. It is obtained as the vertical sum of Na^+'s IV-curve and K^+'s IV-curve. The result may not be a function of V or I as shown but instead described implicitly by an equation such as Eq.(7). $\bar{E}_P$ is the joint passive resting potential at which the current sum from the constituent IV-curves is zero.

is exactly the serial conductor-diffusor IV-curve of the passive Na^+ channel. Now combining the $V_C, I_{Na,p}$ equations and those for the active pumps (9), the system for circuit Fig.3(b) is

$$\begin{cases} CV_C{}' = -[I_{Na,p} + f_K(V_C - \bar{E}_K) + A_{Na} - A_K - I_{ext}] \\ A_{Na}{}' = \lambda A_{Na}[V_C - \gamma(A_{Na} - A_K)] \\ A_K{}' = \lambda A_K[-V_C + \gamma(A_{Na} - A_K)] \\ \epsilon I_{Na,p}{}' = V_C - \bar{E}_{Na} - h_{Na}(I_{Na,p}). \end{cases} \tag{13}$$

In terms of the net and absolute active currents I_A, I_S from Eq.(10), the same system becomes

$$\begin{cases} CV_C{}' = -[I_{Na,p} + f_K(V_C - \bar{E}_K) + I_A - I_{ext}] \\ I_A{}' = \lambda I_S[V_C - \gamma I_A] \\ I_S{}' = \lambda I_A[V_C - \gamma I_A] \\ \epsilon I_{Na,p}{}' = V_C - \bar{E}_{Na} - h_{Na}(I_{Na,p}). \end{cases} \tag{14}$$

The equivalent systems of equations for circuit Fig.3(c) and circuit Fig.3(d) can be derived similarly and they are listed in Table 2.

2.7. Piecewise Linear IV-Characteristics. We are now ready to specify a functional form for the conductive and diffusive IV-curves, Eq.(2, 4), for the purposes of analyzing and simulating the circuit equations. As illustrations, we use continuous and piecewise linear functions for all conductive and diffusive IV-curves, and show later how to generalize the construction to smooth functionals. The functions are listed in Table 3.

We first describe the N-shaped IV-curve for the passive K^+ channel. The component conduc-

tive and diffusive curves are given as follows in their canonical forms.

$$I = f_{\mathrm{K,e}}(V) = g_{\mathrm{K}} V, \text{ with } g_{\mathrm{K}} > 0$$

$$I = f_{\mathrm{K,d}}(V) = \begin{cases} 0 & \text{if } V < v_1 \\ d_{\mathrm{K}}(V - v_1) & \text{if } v_1 < V < v_2, \\ d_{\mathrm{K}}(v_2 - v_1) & \text{if } v_2 < V \end{cases} \quad \text{with } d_{\mathrm{K}} < 0,\ 0 < v_1 < v_2.$$

Here parameter g_{K} is the conductance of K^+'s electro channel and the $r_{\mathrm{K}} = 1/g_{\mathrm{K}}$ is the corresponding resistance, and parameter $d_{\mathrm{K}} < 0$ is K^+'s maximal diffusive coefficient. It is easy to see from Fig.4(a) that the IV-curve for the parallel conductor-diffusor, $I = f_{\mathrm{K,e}}(V) + f_{\mathrm{K,d}}(V)$, is N-shaped if and only if the diffusor can dominate in the range $[v_1, v_2]$ in the following sense,

$$g_{\mathrm{K}} + d_{\mathrm{K}} < 0 \text{ with } g_{\mathrm{K}} > 0, d_{\mathrm{K}} < 0. \tag{15}$$

When this condition is satisfied, the N-shaped parallel conductor-diffusor combo has the designated critical points $V = v_1$ and $V = v_2$ with the middle diffusive branch having a negative slope, $g_{\mathrm{K}} + d_{\mathrm{K}}$. In practical terms, there is a net concentration-dominating intracellular current if the potential difference across the parallel conductor-diffusor is in the range of $[v_1, v_2]$.

For an easier access to numerical simulation and a simpler notation, we will use a `Matlab` notation for Heaviside-type functions as follows

$$(a < x < b) = \begin{cases} 0 & \text{if } x < a \text{ or } b < x \\ 1 & \text{if } a < x < b \end{cases}$$

where a, b are parameters with $-\infty \le a < b \le +\infty$. If either $a = -\infty$ or $b = +\infty$, we simply write $(x < b)$ or $(a < x)$, respectively. Now K^+'s parallel conductor-diffusor can be expressed as

$$I = f_{\mathrm{K}}(V) = f_{\mathrm{K,e}}(V) + f_{\mathrm{K,d}}(V) = g_{\mathrm{K}} V + d_{\mathrm{K}}(V - v_1)(v_1 < V < v_2) + d_{\mathrm{K}}(v_2 - v_1)(v_2 < V). \tag{16}$$

Na^+'s serial conductor-diffusor IV-curve can be similarly constructed. Specifically, we have

$$V = h_{\mathrm{Na,e}}(I) = \frac{1}{g_{\mathrm{Na}}} I, \text{ with } g_{\mathrm{Na}} > 0, \text{ and}$$

$$V = h_{\mathrm{Na,d}}(I) = \begin{cases} 0 & \text{if } I < i_1 \\ \frac{1}{d_{\mathrm{Na}}}(I - i_1) & \text{if } i_1 < I < i_2, \\ \frac{1}{d_{\mathrm{Na}}}(i_2 - i_1) & \text{if } i_2 < I \end{cases} \quad \text{with } d_{\mathrm{Na}} < 0,\ 0 < i_1 < i_2.$$

and in terms of the `Matlab` notation,

$$\begin{aligned} V = h_{\mathrm{Na}}(I) &= h_{\mathrm{Na,e}}(I) + h_{\mathrm{Na,d}}(I) \\ &= \tfrac{1}{g_{\mathrm{Na}}} I + \tfrac{1}{d_{\mathrm{Na}}}(I - i_1)(i_1 < I < i_2) + \tfrac{1}{d_{\mathrm{Na}}}(i_2 - i_1)(i_2 < I). \end{aligned} \tag{17}$$

The V-to-I slope of the middle diffusive branch is

$$\frac{1}{1/g_{\mathrm{Na}} + 1/d_{\mathrm{Na}}} = \frac{g_{\mathrm{Na}} d_{\mathrm{Na}}}{g_{\mathrm{Na}} + d_{\mathrm{Na}}},$$

Table 3: IV-Characteristic Curves

	S-Nonlinearity	N-Nonlinearity
$\mathrm{pK}^{+}_{-}\mathrm{sNa}^{+}_{+}$	$V = h_{\mathrm{Na}}(I)$	$I = f_{\mathrm{K}}(V)$
	• piecewise linear curve: $V = \dfrac{1}{g_{\mathrm{Na}}} I + \dfrac{1}{d_{\mathrm{Na}}}(I - i_1)(i_1 < I < i_2)$ $+\dfrac{1}{d_{\mathrm{Na}}}(i_2 - i_1)(i_2 < I)$ • smooth curve: $V = \dfrac{1}{g_{\mathrm{Na}}} I + \dfrac{1}{d_{\mathrm{Na}}} \rho \tan^{-1} \dfrac{I - i_m}{\rho}$ $+\dfrac{1}{d_{\mathrm{Na}}} \rho \tan^{-1} \dfrac{i_m}{\rho}$, with $i_m = \dfrac{i_1 + i_2}{2},\ \rho = \dfrac{i_2 - i_1}{2} \sqrt{\dfrac{\lvert d_{\mathrm{Na}} \rvert}{g_{\mathrm{Na}} + d_{\mathrm{Na}}}}$	$I = g_{\mathrm{K}} V + d_{\mathrm{K}}(V - v_1)(v_1 < V < v_2)$ $+d_{\mathrm{K}}(v_2 - v_1)(v_2 < V)$ $I = g_{\mathrm{K}} V + d_{\mathrm{K}} \mu \tan^{-1} \dfrac{V - v_m}{\mu}$ $+d_{\mathrm{K}} \mu \tan^{-1} \dfrac{v_m}{\mu}$, with $v_m = \dfrac{v_1 + v_2}{2},\ \mu = \dfrac{v_2 - v_1}{2} \sqrt{\dfrac{g_{\mathrm{K}}}{\lvert g_{\mathrm{K}} + d_{\mathrm{K}} \rvert}}$
$\mathrm{pNa}^{+}_{+}\mathrm{sK}^{+}_{-}$	$V = h_{\mathrm{K}}(I)$	$I = f_{\mathrm{Na}}(V)$
	piewise linear curve: $V = \dfrac{1}{g_{\mathrm{K}}} I + \dfrac{1}{d_{\mathrm{K}}}(I - i_1)(i_1 < I < i_2)$ $+\dfrac{1}{d_{\mathrm{K}}}(i_2 - i_1)(i_2 < I)$	$I = g_{\mathrm{Na}} V + d_{\mathrm{Na}}(v_1 - v_2)(V < v_1)$ $+ d_{\mathrm{Na}}(V - v_2)(v_1 < V < v_2)$
	Conditions: $g_{\mathrm{J}} > 0,\ d_{\mathrm{J}} < 0,\ g_{\mathrm{J}} + d_{\mathrm{J}} > 0$ with $\mathrm{J} = \mathrm{Na},\ \mathrm{or}\ \mathrm{K}$	Conditions: $g_{\mathrm{J}} > 0,\ d_{\mathrm{J}} < 0,\ g_{\mathrm{J}} + d_{\mathrm{J}} < 0$ with $\mathrm{J} = \mathrm{Na},\ \mathrm{or}\ \mathrm{K}$

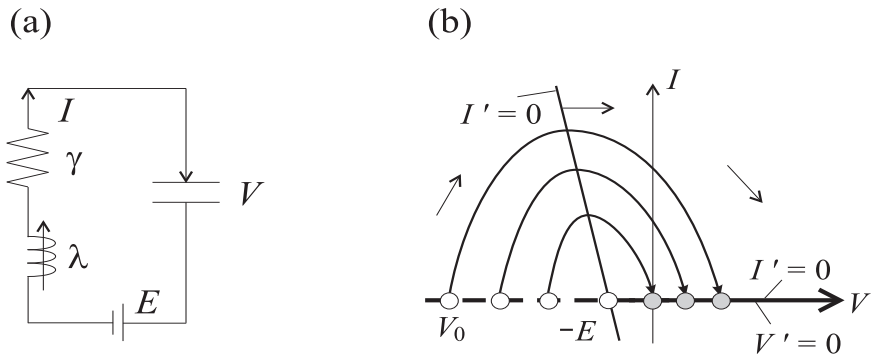

Figure 5: (a) A minimum circuit for the dynamics of a pump. (b) The phase plane portrait of the circuit equation.

which will results in an S-nonlinearity if and only if the slope is negative or equivalently

$$g_{\rm Na} + d_{\rm Na} > 0 \text{ with } g_{\rm Na} > 0, d_{\rm Na} < 0. \tag{18}$$

In such a case, $I = i_1, i_2$ are two critical values, and in practical terms, there is a net concentration-dominating depolarizing voltage across the serial conductor-diffusor if the outward current increases in the range of $[i_1, i_2]$. See Fig.4(b).

3. Circuit Properties. The analysis carried out below is for the equivalent circuit equations Eqs.(13, 14) and those listed in Table 2 with the continuous and piecewise linear IV-curves (16, 17). For the existence of steady states, the S-nonlinearity and the N-nonlinearity are not needed but only their primary conductive branches. For the generation of action potentials, Na^+'s S-nonlinearity is not needed but its primary conductive branch which can alter K^+'s N-nonlinearity qualitatively but only for large conductance. For the generation of spike-bursts, both nonlinearities are required. In all types of the behaviors, the ion pump dynamics are indispensable.

3.1. Pump Dynamics. We begin with the analysis of a minimum circuit consisting of a capacitor, a resister, and a pump in series. The circuit and its phase plane portrait are shown in Fig.5. In particular, the corresponding ordinary differential equations are given as follows

$$\begin{cases} CV' = I \\ I' = \lambda I(-V - E - \gamma I). \end{cases} \tag{19}$$

The V-axis consists of entirely equilibrium points for which those with $V < E$ are unstable and those with $V > E$ are stable. Also, every unstable one is connected to a stable one. This means the following. Suppose that there is initially a net charge q_0 deposited on the lower side of the capacity so that $V_0 = -q_0/C < -E$ and $I = 0$. Then because the equilibrium point $(V_0, 0)$ is unstable and the region $I < 0$ is forbidden, soon or later the pump starts to work when $I(t_0) > 0$ at some time t_0, setting off the transport of the right amount of charges to the top side of the capacitor, and the circuit dynamics eventually settles down at the equilibrium point $(V(+\infty), 0)$. (In the case that the resistance $\gamma = 0$, the equilibrium point can be expressed explicitly as $V(+\infty) = -2E - V_0$, see

below.) This shows that our assumed pump characteristic Eq.(1) indeed captures what we think a pump should do qualitatively — to transport and store up charges unidirectionally.

Analytically, the minimum pump circuit equation Eq.(19) can be solved explicitly by changing it first to its phase equation as below

$$\frac{dI}{dV} = -\lambda C\gamma I - \lambda C(V+E),$$

whose solution with initial condition $I(0) = I_0 > 0, V(0) = V_0$ is

$$I = \left[I_0 + \frac{1}{\gamma}(V_0+E) - \frac{1}{\lambda C\gamma^2}\right]\exp(-\lambda C\gamma[V-V_0]) - \frac{1}{\gamma}(V+E) + \frac{1}{\lambda C\gamma^2}.$$

In the limit $\gamma \to 0$, the solution is on a parabola

$$I = I_0 + \frac{\lambda C}{2}\left[(V_0+E)^2 - (V+E)^2\right] = I_0 + \frac{\lambda C}{2}(V_0-V)(V+V_0+2E).$$

With the limiting initial equilibrium $\lim_{t\to 0^+} I(t) = I_0 = 0, \lim_{t\to 0^+} V(t) = V_0$, the stable equilibrium point opposite to $V_0 < 0$ is $-V_0 - 2E$ as pointed out above.

Dynamics of subcomponents of the circuit equations Eqs.(13, 14), especially those without the pumps, can be considered similarly, but they are well-understood elementary circuits which can be found in almost all undergraduate textbooks for circuitry.

3.2. Passive and Active Resting Potentials. We now consider the whole circuit equations with the piecewise linear IV-curves (16, 17). The steady state equilibriums considered now are all stable. They lie on the primary conductive branches of both ions' passive IV-curves, with the diffusive effect of inward ion flow not dominating these steady states. Hence, the result of this subsection does not depend on Hypothesis (1) and Hypothesis (2) of the two models. In other words, it is the primary feature of a $\mathrm{cK}^+_-\mathrm{cNa}^+_+$ model. For this reason, we will restrict the effective range to the primary conductive branches and assume instead the following

$$I_{\mathrm{K,p}} = f_{\mathrm{K}}(V_{\mathrm{C}} - \bar{E}_{\mathrm{K}}) = g_{\mathrm{Na}}(V_{\mathrm{C}} - \bar{E}_{\mathrm{K}}) \text{ and } V_{\mathrm{C}} = h_{\mathrm{Na}}(I_{\mathrm{Na,p}}) + \bar{E}_{\mathrm{Na}} = \frac{1}{g_{\mathrm{Na}}} I_{\mathrm{Na,p}} + \bar{E}_{\mathrm{Na}}$$

We will also use the following notation interchangeably for resistance and conductance

$$g_{\mathrm{K}} = \frac{1}{r_{\mathrm{K}}},\ \ g_{\mathrm{Na}} = \frac{1}{r_{\mathrm{Na}}},\ \ g_{\mathrm{A}} = \frac{1}{\gamma},\ \ g_{\mathrm{P}} = g_{\mathrm{K}} + g_{\mathrm{Na}}.$$

Under the restriction to primary conductive branches, the active membrane equilibrium point, $V_{\mathrm{C}}{}' = I_{\mathrm{A}}{}' = I_{\mathrm{S}}{}' = I_{\mathrm{Na,p}}{}' = 0$, is solved from the following equations using the equivalent circuit equation (14):

$$\begin{cases} I_{\mathrm{Na,p}} + I_{\mathrm{K,p}} + I_{\mathrm{A}} - I_{\mathrm{ext}} = 0 \\ V_{\mathrm{C}} - \gamma I_{\mathrm{A}} = 0 \\ I_{\mathrm{K,p}} = g_{\mathrm{Na}}(V_{\mathrm{C}} - \bar{E}_{\mathrm{K}}) \\ V_{\mathrm{C}} = r_{\mathrm{Na}} I_{\mathrm{Na,p}} + \bar{E}_{\mathrm{Na}}. \end{cases} \tag{20}$$

It is a linear system, simple to solve exactly. Several cases are considered below.

We first consider the equilibrium states when one of the ions is blocked. When K^+ is blocked, the equilibrium for the reduced Na^+-system, i.e. the cNa^+_+ model, is solved from the same equation (20) with the third equation deleted and the K^+-currents set to zeroes $I_{\rm K,p} = A_{\rm K} = 0$ in the first equation. The reduced system becomes,

$$\begin{cases} I_{\rm Na,p} + A_{\rm Na} - I_{\rm ext} = 0 \\ V_{\rm C} - \gamma A_{\rm Na} = 0 \\ V_{\rm C} = r_{_{\rm Na}} I_{\rm Na,p} + \bar{E}_{\rm Na}, \end{cases}$$

Since there are 4 variables, $V_{\rm C}, I_{\rm Na,p}, A_{\rm Na}$, and $\bar{E}_{\rm Na}$ to determine from 3 equations, one of the 4 variables can be used to determine the others. Solutions to the equations can be explicitly expressed as follows:

$$\begin{aligned} &V_{\rm C} = E_{\rm Na} := \frac{g_{\rm Na}}{g_{\rm Na} + g_{_{\rm A}}} \bar{E}_{\rm Na} + \frac{1}{g_{\rm Na} + g_{_{\rm A}}} I_{\rm ext} \\ &A_{\rm Na} = g_{_{\rm A}} E_{\rm Na} \\ &I_{\rm Na,p} = -g_{_{\rm A}} E_{\rm Na} + I_{\rm ext}. \end{aligned} \tag{21}$$

Since $A_{\rm Na} > 0$ for the pump current, for the K^+-blocked system to have an active membrane resting potential (with external forcing $I_{\rm ext} = 0$) we must have from the second expression that

$$E_{\rm Na} > 0$$

which also gives the same polarity to the passive resting potential $\bar{E}_{\rm Na} > 0$ from the first expression when $I_{\rm ext} = 0$. Notice from Eq.(21) above, that when the voltage is clamped at zero, $V_C = E_{\rm Na} = 0$, the external current is $I_{\rm ext} = -g_{_{\rm Na}} \bar{E}_{\rm Na}$, that is, the passive resting potential can be measured if the conductance $g_{_{\rm Na}}$ is known.

For the Na^+-blocked equilibrium, the analysis is exactly the same for the reduced pK^+_- system. Specifically, after deleting the fourth equation in (20), setting $I_{\rm Na,p} = A_{\rm Na} = 0$, and dividing the third equation by $g_{_{\rm Na}}$ and equating the role of $-A_{\rm K}$ to that of $A_{\rm Na}$, the equation form is exactly the same as the K^+-blocked equilibrium equations above. As a result, K^+'s active resting potential can be solved as

$$E_{\rm K} = \frac{g_{\rm K}}{g_{\rm K} + g_{_{\rm A}}} \bar{E}_{\rm K} + \frac{1}{g_{\rm K} + g_{_{\rm A}}} I_{\rm ext}. \tag{22}$$

Again, with $I_{\rm ext} = 0$, both $E_{\rm K}$ and $\bar{E}_{\rm K}$ have the same polarity and the corresponding ion pump equilibrium current is

$$A_{\rm K} = -g_{_{\rm A}} E_{\rm K}$$

in order for which to be positive we must have $E_{\rm K} < 0$. Similarly, the passive resting potential $\bar{E}_{\rm K}$ can be measured from an equilibrium which is voltage-clamped at zero when $g_{\rm K}$ is known:

$$V_{\rm C} = E_{\rm K} = 0, \ \bar{E}_{\rm K} = \frac{1}{g_{\rm K}} I_{\rm ext}.$$

The result above is summarized below.

Proposition 1. *For both the* $\mathrm{pK}^+_-\mathrm{sNa}^+_+$ *and* $\mathrm{pNa}^+_+\mathrm{sK}^+_-$ *models, the directionality of an ion species' pump from Hypothesis 4 determines the polarity of the ion species' active resting potential from Hypothesis 3, which in turn implies the same polarity for the ion species' passive resting potential. Also,* $\bar{E}_{\mathrm{Na}}$ *(resp.* $\bar{E}_{\mathrm{K}}$*) can be measured by the external current if the voltage is clamped at zero and* K^+ *(resp.* Na^+*) is blocked.*

Note that this result can be easily generated to other ions' resting potentials. For example, if the cell has a Cl^- ion pump and has $E_{\mathrm{Cl}} < 0$, the same polarity as E_{K}, then the cell should pump Cl^- ion outward, in the opposite direction to K^+'s pump direction. This is because Cl^- is negative charged whereas K^+ is positive charged, but both result in a net inward pump current to which the same analysis above then applies. Similarly, $E_{\mathrm{Cl}} > 0$ iff Cl^- is pumped inward.

Now consider the full steady state equilibrium from equation (20) without any ion blockage. Upon simplification, it is straightforward to derive or to check that the active membrane resting potential is

$$E_{\mathrm{m}} = \frac{g_{\mathrm{Na}}\bar{E}_{\mathrm{Na}} + g_{\mathrm{K}}\bar{E}_{\mathrm{K}}}{g_{\mathrm{Na}} + g_{\mathrm{K}} + g_{\mathrm{A}}} + \frac{1}{g_{\mathrm{Na}} + g_{\mathrm{K}} + g_{\mathrm{A}}} I_{\mathrm{ext}}. \tag{23}$$

This relation has several equivalent form. First, the total passive resting potential $\bar{E}_{\mathrm{P}}$ introduced in (6) is another conductance-weighted linear combination of the passive resting potentials of both ions:

$$\bar{E}_{\mathrm{P}} = \frac{g_{\mathrm{Na}}\bar{E}_{\mathrm{Na}} + g_{\mathrm{K}}\bar{E}_{\mathrm{K}}}{g_{\mathrm{Na}} + g_{\mathrm{K}}},$$

see Fig.4(c) for an illustration and derivation. With this relation, the active membrane resting potential is

$$E_{\mathrm{m}} = \frac{g_{\mathrm{P}}}{g_{\mathrm{P}} + g_{\mathrm{A}}}\bar{E}_{\mathrm{P}} + \frac{1}{g_{\mathrm{P}} + g_{\mathrm{A}}} I_{\mathrm{ext}}.$$

Also, using the relations obtained above between the active and passive resting potentials of both ions, it can be expressed as another conductance-weighted average of active resting potentials,

$$\begin{aligned} E_{\mathrm{m}} &= \frac{g_{\mathrm{Na}}\bar{E}_{\mathrm{Na}} + g_{\mathrm{K}}\bar{E}_{\mathrm{K}}}{g_{\mathrm{Na}} + g_{\mathrm{K}} + g_{\mathrm{A}}} + \frac{1}{g_{\mathrm{Na}} + g_{\mathrm{K}} + g_{\mathrm{A}}} I_{\mathrm{ext}} \\ &= \frac{(g_{\mathrm{Na}} + g_{\mathrm{A}})E_{\mathrm{Na}} + (g_{\mathrm{K}} + g_{\mathrm{A}})E_{\mathrm{K}}}{g_{\mathrm{Na}} + g_{\mathrm{K}} + g_{\mathrm{A}}} + \frac{3}{g_{\mathrm{Na}} + g_{\mathrm{K}} + g_{\mathrm{A}}} I_{\mathrm{ext}} \\ &= \frac{g_{\mathrm{Na}}E_{\mathrm{Na}} + g_{\mathrm{K}}E_{\mathrm{K}} + g_{\mathrm{A}}E_{\mathrm{A}}}{g_{\mathrm{Na}} + g_{\mathrm{K}} + g_{\mathrm{A}}} + \frac{3}{g_{\mathrm{Na}} + g_{\mathrm{K}} + g_{\mathrm{A}}} I_{\mathrm{ext}}, \end{aligned} \tag{24}$$

where E_{A} is simply defined as the sum of the active resting potentials of the ions: $E_{\mathrm{A}} = E_{\mathrm{Na}} + E_{\mathrm{K}}$.

As a concluding note, we recall that the nullcline for the total absolute active current I_{S} equation coincides that of the net active current's nullcline, $V_{\mathrm{C}} - \gamma I_{\mathrm{A}} = 0$. As a result, the membrane steady state equilibrium is not dynamically fixed. In fact, the resting potentials form a line parallel with the I_{S}-axis in the observable state space of $(V_{\mathrm{C}}, I_{\mathrm{C}} + I_{\mathrm{Na,p}} + I_{\mathrm{K,p}} + I_{\mathrm{A}})$ of the circuit. This is a new and interesting property:

Proposition 2. *For both the* $\mathrm{pK}^+_-\mathrm{sNa}^+_+$ *and* $\mathrm{pNa}^+_+\mathrm{sK}^+_-$ *models, the membrane can maintain the same observable steady state by pumping the potassium and sodium ions at different individual rates as long as the ion pump maintains the same net active current* I_{A} *at the corresponding steady state rate. Also, the conductance weighted passive resting potentials can be measured by the external current when the membrane potential is clamped at zero:* $g_{\mathrm{Na}}\bar{E}_{\mathrm{Na}} + g_{\mathrm{K}}\bar{E}_{\mathrm{K}} = I_{\mathrm{ext}}$.

More importantly, this continuum of equilibrium states are structurally stable to be shown later, the sole consequence to the existence of the dual ion pumps. In this case, changing the total absolute current I_{S} can leave the steady state fixed. In contrast, we will show in [12] that the opposite happens when seemingly stable action potentials and spike-bursts change extremely slowly with varying I_{S}, the phenomena of metastability and plasticity.

3.3. Action Potential Generation With Ion Blockage. We now consider the neuron models with either the sodium ion or the potassium ion blocked, i.e. the pK^+_- or the sNa^+_+ subsystem, respectively. For the first case, $I_{\mathrm{Na,p}} = A_{\mathrm{Na}} = 0$, the reduced model equation (13) becomes

$$\begin{cases} CV_{\mathrm{C}}{}' = -[f_{\mathrm{K}}(V_{\mathrm{C}} - \bar{E}_{\mathrm{K}}) - A_{\mathrm{K}} - I_{\mathrm{ext}}] \\ A_{\mathrm{K}}{}' = \lambda A_{\mathrm{K}}[-V_{\mathrm{C}} - \gamma A_{\mathrm{K}}]. \end{cases} \tag{25}$$

It is a 2-dimensional system in $V_{\mathrm{C}}, A_{\mathrm{K}}$. As shown in (15), for $g_{\mathrm{K}} + d_{\mathrm{K}} < 0$, K^+'s IV-curve admits an N-shaped nonlinearity. As a result, the system above behaves similarly like the FitzHugh-Nagumo equations, see Fig.6(a) for a phase plane illustration. However, unlike the FitzHugh-Nagumo equations, the effective range of the Na^+-blocked K^+-system is restricted to the upper half plane $A_{\mathrm{K}} > 0$ since the V_{C}-axis, $A_{\mathrm{K}} = 0$, is invariant for the system through which no solutions originated above can cross. Because of the fact that A_{K}'s nontrivial nullcline, $A_{\mathrm{K}} = -V_{\mathrm{C}}/\gamma$, lies only in the second quadrant, any active equilibrium state E_{K} with $A_{\mathrm{K}} > 0$ must be negative. From the phase portrait, we can clearly see that the active equilibrium point is a stable node while the passive equilibrium point is a saddle, which is stable only in the complete absence of active current $A_{\mathrm{K}} = 0$. Also, we can see that the passive resting potential $\bar{E}_{\mathrm{K}}$ is always smaller than the active resting potential E_{K}, both are related by Eq.(22).

The phase portrait Fig.6(a) shows a stable active equilibrium state base with $I_{\mathrm{ext}} = 0$ as well as a nonstable active equilibrium state case with a positive $I_{\mathrm{ext}} > 0$ for which a limit cycle emerges. For the limit cycle case to occur, two conditions need to hold: (i) the critical voltage value for the N-nonlinearity must be negative, $\bar{E}_{\mathrm{K}} + v_1 < 0$, and (ii) the combined diffusive coefficient, $g_{\mathrm{K}} + d_{\mathrm{K}} < 0$, must not be too large in magnitude so that the two critical A_{K}-current values of the N-nonlinearity lie entirely above the V_{C}-axis.

The active steady state is stable for a range of I_{ext} and it gives rise to an I_{ext}-forced limit cycle, or action potential, when it loses its stability. The I_{ext}-threshold for the action potentials is determined when the active resting potential equilibrium E_{K} crosses the first critical value of the N-shaped IV-curve at $v_1 + \bar{E}_{\mathrm{K}}$ into the diffusion-dominating region. Solving from the equation

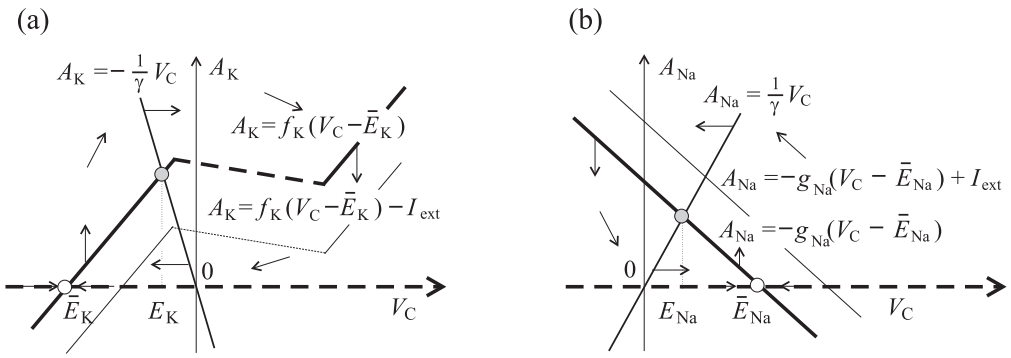

Figure 6: (a) Na^+-blocked phase portrait. (b) K^+-blocked phase portrait. It is clear from the phase portraits that active resting potentials do not always exist if $\bar{E}_{\rm K} > 0$ or $\bar{E}_{\rm Na} < 0$.

(22) and the threshold condition $E_{\rm K} = v_1 + \bar{E}_{\rm K}$, we have the threshold value

$$I_{\rm ext} > I_{\rm K,thr} := \frac{\gamma}{1+g_{\rm K}r}\left[v_1 + \frac{1}{1+g_{\rm K}\gamma}\bar{E}_{\rm K}\right],$$

which is small for small γ. It implies that action potentials can be readily generated for modest external forcing. The type of action potentials are K^+-mediated. This result can be summarized as follows.

Proposition 3. *For the* Na^+*-blocked* $pK^{\pm}_{-}sNa^{+}_{+}$ *model, the* K^+*-mediated action potentials can be readily generated for* $I_{\rm ext} > I_{\rm K,thr}$ *if* $\gamma > 0,\ g_{\rm K} + d_{\rm K} < 0$ *are relatively small in magnitude each, and if the left critical value of the* N*-nonlinearity in voltage is negative,* $\bar{E}_{\rm K} + v_1 < 0$*. However, when* $\bar{E}_{\rm K} + v_1 > 0$*, no amount of stimuli* $I_{\rm ext}$ *can induce* K^+*-mediated action potentials. For the* K^+*-blocked* $pNa^{+}_{+}sK^{+}_{-}$ *model, the* Na^+*-mediated action potentials can be readily generated when* $\bar{E}_{\rm Na} + v_1 < 0$ *or* $\bar{E}_{\rm Na} + v_1 > 0$ *but small because of the smallness of the ion pump's resistance* γ*.*

We now consider the K^+-blocked model of Eq.(13),

$$\begin{cases} CV_{\rm C}{}' = -[I_{\rm Na,p} + A_{\rm Na} - I_{\rm ext}] \\ A_{\rm Na}{}' = \lambda A_{\rm Na}[V_{\rm C} - \gamma A_{\rm Na}] \\ \epsilon I_{\rm Na,p}{}' = V_{\rm C} - \bar{E}_{\rm Na} - h_{\rm Na}(I_{\rm Na,p}). \end{cases} \tag{26}$$

In the case that the active resting potential does not lie on Na^+'s diffusive branch, we can consider the system restricted on its primary conductive branch as before. For the piecewise linear case, the primary branch of the $I_{\rm Na,p}$-nullcline is $0 = V_{\rm C} - \bar{E}_{\rm Na} - h_{\rm Na}(I_{\rm Na,p}) = V_{\rm C} - \bar{E}_{\rm Na} - r_{_{\rm Na}} I_{\rm Na,p}$, from which

$$I_{\rm Na,p} = g_{_{\rm Na}}(V_{\rm C} - \bar{E}_{\rm Na}).$$

Substitute it into Eq.(26) gives the reduced 2-dimensional system

$$\begin{cases} CV_{\rm C}{}' = -[g_{_{\rm Na}}(V_{\rm C} - \bar{E}_{\rm Na}) + A_{\rm Na} - I_{\rm ext}] \\ A_{\rm Na}{}' = \lambda A_{\rm Na}[V_{\rm C} - \gamma A_{\rm Na}]. \end{cases}$$

It can be seen from its phase portrait Fig.6(b) the following: the system is restricted to the upper half plane $A_{\rm Na} \geq 0$; if exists the active resting potential $E_{\rm Na}$ must be positive; and only in the absence of the active pump current $A_{\rm Na} = 0$ is Na^+'s passive resting potential $\bar{E}_{\rm Na}$ stable; and the relationship $0 < E_{\rm Na} < \bar{E}_{\rm Na}$ must hold as concluded already from the last subsection. Also, when restricted on the primary conductive branch, the active resting potential $E_{\rm Na}$ has been solved explicitly in (21) as

$$V_{\rm C} = E_{\rm Na} = \frac{\gamma g_{\rm Na}}{1+\gamma g_{\rm Na}} \bar{E}_{\rm Na} + \frac{\gamma}{1+\gamma g_{\rm Na}} I_{\rm ext}.$$

and $A_{\rm Na} = E_{\rm Na}/\gamma > 0,\ I_{\rm Na,p} = -A_{\rm Na} + I_{\rm ext}$.

In order for the neuron to generate action potentials, i.e. for the circuit to oscillate, the active resting potential equilibrium needs to lose its stability. For this to happen, it have to enter Na^+'s diffusive branch of its passive IV-curve $V_{\rm C} = h_{\rm Na}(I_{\rm Na,p}) + \bar{E}_{\rm Na}$ through the lower critical point $I_{\rm Na,p} = i_1$. Using this relation to determine the needed external forcing threshold from the equation $i_1 = I_{\rm Na,p} = -A_{\rm Na} + I_{\rm ext} = -E_{\rm Na}/\gamma + I_{\rm ext}$, we have

$$I_{\rm ext} > I_{\rm Na,thr} := \frac{1+\gamma g_{\rm Na}}{\gamma g_{\rm Na}} i_1 + \frac{1}{\gamma} \bar{E}_{\rm Na}.$$

For fixed i_1 and $\bar{E}_{\rm Na}$ but small γ, this threshold can be too large a current to be injected to the neuron to realistically generate K^+-blocked, Na^+-mediated action potentials, in contrast to the relative ease to generate Na^+-blocked, K^+-mediated action potentials as shown above. In summary, we have the following.

Proposition 4. *For the* K^+*-blocked* $pK^+_-sNa^+_+$ *model,* Na^+*-mediated action potentials cannot be easily generated with modest external forcing since it needs* $I_{\rm ext} > I_{\rm Na,thr}$ *but* $\lim_{\gamma\to 0^+} I_{\rm Na,thr} = \infty$. *For* $I_{\rm ext} < I_{\rm Na,thr}$ *the circuit settles down at a stable equilibrium whose corresponding resting potential* $E_{\rm Na}$ *is always positive. The same is true for* K^+*-mediated action potentials in the* Na^+*-blocked* $pNa^+_+sK^+_-$ *model.*

3.4. Action Potentials Without Ion Blockage. We now consider a configuration between K^+'s N-characteristic curve and Na^+'s S-characteristic curve in such a way that the diffusive branch of Na^+'s IV-curve does not affect the circuit dynamics, i.e. the $K^+_-cNa^+_+$ model. The following notation is used, see Fig.7,

$$\begin{aligned} &k_1 = f_{\rm K}(v_1) = f_{\rm K}(v_1^*), \text{ with } v_1 < v_1^*, \text{ and } k_2 = f_{\rm K}(v_2^*) = f_{\rm K}(v_2), \text{ with } v_2^* < v_2 \\ &n_1 = h_{\rm Na}(i_1) = h_{\rm Na}(i_1^*), \text{ with } i_1 < i_1^*, \text{ and } n_2 = h_{\rm Na}(i_2^*) = h_{\rm Na}(i_2), \text{ with } i_2^* < i_2 \end{aligned}$$

The oriented loop with vertices $(v_1,k_1),(v_1^*,k_1),(v_2,k_2),(v_2^*,k_2)$ hugging K^+'s IV-curve is called K^+'s *hysteresis* loop. Similarly, the oriented loop with vertices $(n_1,i_1),(n_1,i_1^*),(n_2,i_2),(n_2,i_2^*)$ hugging Na^+'s IV-curve is called Na^+'s hysteresis loop. We note that whether or not an IV-curve forms an hysteresis is context-dependent. Take the K^+'s N-shaped IV-curve $I = f_{\rm K}(V)$ as an example. As the nullcline for the equation $V' = I - f_{\rm K}(V)$, the curve forms an hysteresis because a V-phase line can intersect the curve multiple times, and the intersecting points on the two end

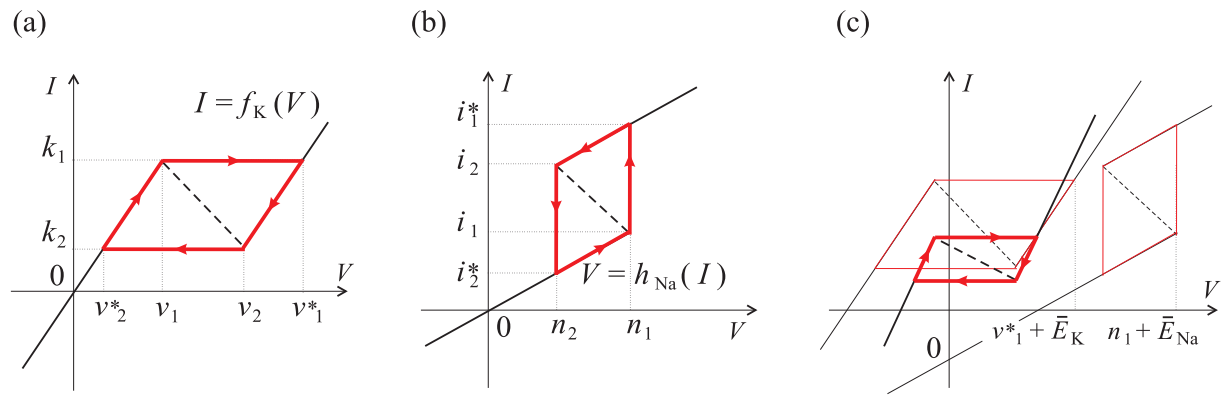

Figure 7: (a) K^+'s hysteresis loop of the $pK^{+}_{-}sNa^{+}_{+}$ model. (b) Na^+'s hysteresis loop of the $pK^{+}_{-}sNa^{+}_{+}$ model. (c) The translated IV-curves by their corresponding passive resting potentials, showing a configuration satisfying condition (27) and condition (28). The new N-hysteresis loop is the result of the vertical sum of K^+'s IV-curve and the primary resistive branch of Na^+'s IV-curve.

branches are stable equilibrium points of the equation and the intersection with the middle branch is an unstable equilibrium point. However, the curve does not form an hysteresis for the equation $I' = I - f_{\rm K}(V)$ because every I-phase line intersects the curve at most once.

Upon translation by their respective passive resting potentials, K^+'s loop is shifted parallel to the V-axis leftwards by $\bar{E}_{\rm K}$ amount and Na^+'s loop is shifted parallel to the V-axis rightwards by $\bar{E}_{\rm Na}$ amount. The mutual configuration of the shifted loops for this subsection is defined by the following condition:

$$v^*_1 + \bar{E}_{\rm K} < n_1 + \bar{E}_{\rm Na}. \tag{27}$$

See Fig.7(c). Under this condition, K^+'s N-characteristic lies in the voltage range, $V < n_1 + \bar{E}_{\rm Na}$, of the primary conductive branch of Na^+'s S-characteristic. As a result, the former will persist if the latter is not too steep in slope, i.e., $g_{\rm Na}$ is modest. More precisely, under the following condition

$$g_{\rm K} + d_{\rm K} + g_{\rm Na} < 0, \tag{28}$$

the combined K^+-Na^+ IV-characteristic, $I = f_{\rm K}(V - \bar{E}_{\rm K}) + g_{\rm Na}(V - \bar{E}_{\rm Na})$, with K^+'s hysteresis loop and Na^+'s primary resistive branch in parallel again permits a new N-shaped IV-curve in the range $V_{\rm C} < n_1 + \bar{E}_{\rm Na}$. That is, K^+'s-diffusive channel not only dominates its own conductive channel in its $[v_1, v_2]$ range, but also dominates the combined passive parallel channels in the same range. In fact, the conductance sum of Eq.(28) is the new diffusive coefficient for the combined IV-curve, see Fig.7(c). When condition (27) is violated, K^+'s N-loop may not persist, as such is a case illustrated in Fig.4(c).

It turns out that under condition (27), the circuit dynamics do not extend into the region beyond $V_{\rm C} > n_1 + \bar{E}_{\rm Na}$ and $I_{\rm Na,p} > i_1$. Hence, we can restrict the analysis to the effective region for Na^+ in $\{V_{\rm C} < n_1 + \bar{E}_{\rm Na},\ I_{\rm Na,p} < i_1\}$. As a result, we only need to consider the primary branch of Na^+'s IV-curve to be $V_{\rm C} - \bar{E}_{\rm Na} = h_{\rm Na}(I_{\rm Na,p}) = r_{\rm Na} I_{\rm Na,p}$ or $I_{\rm Na,p} = g_{\rm Na}(V_{\rm C} - \bar{E}_{\rm Na})$ as we have done for

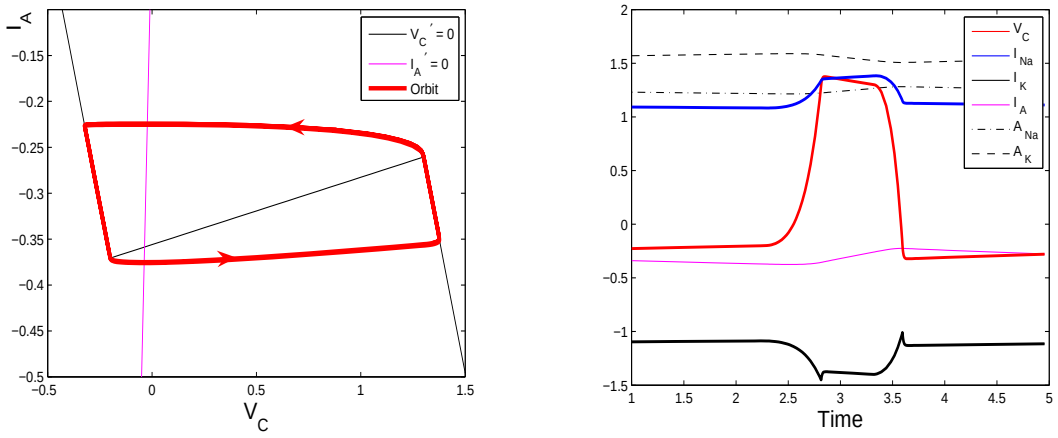

(a) (b)

Figure 8: Dimensionless simulations of Eq.(14) with parameter values: $g_{\rm Na} = 0.17,\ d_{\rm Na} = -0.06,\ i_1 = 0.5,\ i_2 = 1,\ \bar{E}_{\rm Na} = 0.6,\ g_{\rm K} = 1,\ d_{\rm K} = -1.25,\ v_1 = 0.5,\ v_2 = 2,\ \bar{E}_{\rm K} = -0.7,\ C = 0.01,\ \lambda = 0.05,\ \gamma = 0.1,\ I_{\rm ext} = 0,\ \epsilon = 0.001$. (a) A phase plane view of the oscillation. (b) A time series plot for which $I_{\rm Na} = I_{\rm Na,p} + A_{\rm Na},\ I_{\rm K} = I_{\rm K,p} + A_{\rm K} = f_{\rm K}(V_{\rm C} - \bar{E}_{\rm K}) + A_{\rm K}$.

condition (28). This restriction solves the last equation of (14) for the ideal situation when $\epsilon = 0$, and as a result, Eq.(14) is reduced to a 3-dimensional system below

$$\begin{cases} CV_{\rm C}{}' = -[g_{\rm Na}(V_{\rm C} - \bar{E}_{\rm Na}) + f_{\rm K}(V_{\rm C} - \bar{E}_{\rm K}) + I_{\rm A} - I_{\rm ext}] \\ I_{\rm A}{}' = \lambda I_{\rm S}[V_{\rm C} - \gamma I_{\rm A}] \\ I_{\rm S}{}' = \lambda I_{\rm A}[V_{\rm C} - \gamma I_{\rm A}]. \end{cases}$$

Because the absolute active current $I_{\rm S}$ can be solved in terms of $V_{\rm C}, I_{\rm A}$ as in (11), and thus decoupled from the first two equations, the system above is essentially 2-dimensional. Fig.8(a) shows a phase portrait in the $V_{\rm C}I_{\rm A}$ space for all $I_{\rm S} > 0$. The inverted N-curve is the $V_{\rm C}$-nullcline

$$I_{\rm A} = -(g_{\rm Na}(V_{\rm C} - \bar{E}_{\rm Na}) + f_{\rm K}(V_{\rm C} - \bar{E}_{\rm K}) - I_{\rm ext}),$$

forming an hysteresis, and the line is the $I_{\rm A}$-nullcline $I_{\rm A} = V_{\rm C}/\gamma$.

Depending on the external forcing current $I_{\rm ext}$, the circuit can have a stable equilibrium point lying on both primary conductive branches of the two ions whose corresponding resting potential is given by formula (23). In order for the neuron to generate action potentials, this steady state resting potential must lose its stability by entering into the combined diffusive branch of the K^+-Na^+ IV-curve through the same left critical point $v_1 + \bar{E}_{\rm K}$ (which remains the same for piecewise IV-curves but may shift for smooth IV-curves.) Hence, the action potential threshold for the external current is solved from $v_1 + \bar{E}_{\rm K} = E_{\rm m}$ and equation (23) as below

$$I_{\rm ext} > I_{\rm m,thr} := (g_{\rm Na} + g_{\rm K} + g_{\rm A})(v_1 + \bar{E}_{\rm K}) - (g_{\rm Na}\bar{E}_{\rm Na} + g_{\rm K}\bar{E}_{\rm K}). \tag{29}$$

Fig.8 shows a simulation of action potentials when the threshold condition above and the configuration conditions (27, 28) are satisfied. A 3-dimensional view of the action potential is also shown

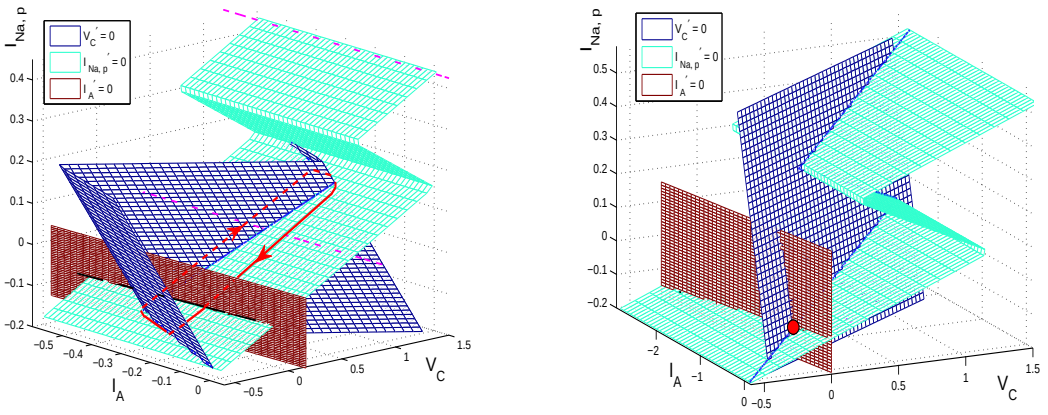

(a) (b)

Figure 9: (a) The action potential cycle on the primary conductive branch of $I_{\mathrm{Na,p}}$-nullcline surface in the $V_{\mathrm{C}}I_{\mathrm{A}}I_{\mathrm{Na,p}}$-space when conditions (27, 28) are satisfied. (b) The same view except for condition (30) or (31). The equilibrium point (filled circle) on both K^+'s primary conductive branch and Na^+'s primary conductive branch is always stable.

in Fig.9(a), showing it lies entirely on the primary branch of $I_{\mathrm{Na,p}}$'s S-shaped nullcline surface. The type of action potentials is K^+-mediated, the result of diffusion domination by K^+ ion only.

Proposition 5. *The* $\mathrm{pK}^+_-\mathrm{sNa}^+_+$ *model can generate* K^+*-mediated action potential oscillations under the conditions (27, 28), which reduce the model to a* $\mathrm{pK}^+_-\mathrm{cNa}^+_+$ *model.*

3.5. Termination of K^+-Mediated Action Potentials. We now consider the case in which K^+'s diffusive channel is either not dominating or completely absent in the effective region of interest. In the non-dominance situation we assume the opposite to condition (28)

$$g_{\mathrm{K}} + d_{\mathrm{K}} + g_{\mathrm{Na}} > 0 \tag{30}$$

for which K^+'s N-characteristic does not persist as in Fig.7(c). In the absence situation we can assume

$$n_1 + \bar{E}_{\mathrm{Na}} < v_1 + \bar{E}_{\mathrm{K}} \tag{31}$$

for which Na^+'s S-characteristic lies in the primary conductive region of K^+'s passive channels.

In both situations, we can assume for simplicity that K^+'s passive IV-characteristic in the effective region of interest to be simply

$$I = f_{\mathrm{K}}(V) = g_{\mathrm{Na}}V.$$

In this case, the system of equations (14) remains 4-dimensional in $V_{\mathrm{C}}, I_{\mathrm{A}}, I_{\mathrm{S}}, I_{\mathrm{Na,p}}$. However, since the I_{S}-equation is decoupled from the rest equations, the nullcline structures of the other variables remain fixed for all values of I_{S}. As a result, the system is essentially 3-dimensional.

Fig.9(b) shows the nullcline surfaces of the $V_{\rm C}I_{\rm A}I_{\rm Na,p}$-system. Adding to this advantageous feature of dimension reduction, the nontrivial part of the $I_{\rm S}$-nullcline coincides with that of $I_{\rm A}$'s. Notice further that because both the $V_{\rm C}$-nullcline and $I_{\rm A}$-nullcline surfaces are planes given as

$$I_{\rm A} = -(I_{\rm Na,p} + g_{\rm K}(V_{\rm C} - \bar{E}_{\rm K}) - I_{\rm ext}) \ \text{ and } \ I_{\rm A} = V_{\rm C}/\gamma, \ \text{respectively,}$$

the relative configuration of these surfaces becomes even simpler as shown. These two planes intersects along a line, which in turn intersects the S-shaped $I_{\rm Na,p}$-nullcline at one, or two, or three points. However, it is straightforward to show that the equilibrium points on the conductive branches are stable and that the one on the diffusive branch is unstable if there are indeed multiple equilibrium points. Fig.9(b) shows the case that there is only one equilibrium point which lies in Na^+'s primary conductive branch. Because of the existence of such stable equilibrium points on Na^+'s conductive branches, action potentials, i.e., oscillations, cannot be generated. When cast in terms of selective blockage of K^+'s diffusive channel, we can state the following:

Proposition 6. *It is not possible to generate* K^+*-mediated action potentials for the* $pK^+_-sNa^+_+$ *model if* K^+*'s diffusive channel is not dominating in the sense that either condition (30) or condition (31) or both hold, in which cases the reduced system is a* cK^+cNa^+ *model.*

3.6. Spike-Burst Generation. We now consider the case in which the combined passive channels from both ions result in an IV-characteristic curve like the one depicted in Fig.4(c). The analytical conditions for the configuration is the following:

(a) The $\bar{E}_{\rm Na}$-shifted Na^+ hysteresis loop lies in the diffusive region of the $\bar{E}_{\rm K}$-shifted K^+ hysteresis loop:

$$v_1 + \bar{E}_{\rm K} < n_2 + \bar{E}_{\rm Na} < n_1 + \bar{E}_{\rm Na} < v_2 + \bar{E}_{\rm K}. \tag{32}$$

(b) K^+'s diffusive channel dominates K^+'s conductive channel and Na^+'s conductive channel combined:

$$g_{\rm K} + d_{\rm K} + g_{\rm Na} < 0. \tag{33}$$

(c) Na^+'s diffusive channel dominates its serial conductive channel in the region $[i_1, i_2]$ to have an S-hysteresis:

$$\frac{1}{g_{\rm Na}} + \frac{1}{d_{\rm Na}} < 0. \tag{34}$$

(d) Burst (action potential) excitation condition:

$$I_{\rm ext} > I_{\rm m,thr} := (g_{\rm Na} + g_{\rm K} + g_{\rm A})(\bar{E}_{\rm K} + v_1) - (g_{\rm Na}\bar{E}_{\rm Na} + g_{\rm K}\bar{E}_{\rm K}). \tag{35}$$

Condition (d) is the same as the action potential threshold condition (29) so that the equilibrium point on the primary conductive branch of Na^+'s is unstable. This condition allows the generation of K^+-mediated action potentials or bursts, a more appropriate term in the context of this subsection. Condition (c) is what it says. Condition (b) is more than enough to guarantee K^+'s IV-curve to have an N-nonlinearity which only requires $g_{\rm K} + d_{\rm K} < 0$. In fact, in K^+'s diffusive range, $[v_1 + \bar{E}_{\rm K}, v_2 + \bar{E}_{\rm K}]$, the combined passive channel from both ions in parallel is still dominated by K^+'s diffusion. This condition is the same as the second condition (28) for the generation of K^+-mediated action potentials or bursts. However, it is the condition (a) that is critical for the generation of spike-bursts considered here. More specifically, it violates the other sufficient condition (27) for the generation of K^+-mediated action potentials to prevent them from completion. This is because the lower knee point of Na^+'s S-hysteresis cuts into the K^+-mediated action potential in K^+'s diffusive range. In another words, at the lower knee of the S-hysteresis, the $I_{\rm Na,p}$-equation takes over and the K^+-mediated burst is interrupted by Na^+-mediated spikes around Na^+'s S-hysteresis.

Fig.10 gives an illustration on the geometric mechanism of spike-burst generation for this model. The mathematical method to study and to understand such problems has developed and matured through a series of works [3, 4, 5, 6, 7, 8, 9, 10]. The key of the method is to utilize the fast-time scale of $I_{\rm Na,p}$'s equation for sufficiently small $\epsilon > 0$. More specifically, at a near ideal situation when $\epsilon \approx 0$, all solutions of the system are quickly equilibrating on the conductive branches of Na^+'s S-hysteresis, thus reducing the analysis to the system restricted to the lower dimensional conductive branches of $I_{\rm Na,p}$'s nullcline surface. Because $I_{\rm S}$'s non-trivial nullcline coincides with $I_{\rm A}$'s nullcline, the analysis is further simplified into a 2-dimensional phase plane analysis of the reduced $V_{\rm C}I_{\rm A}$-subsystem on the two branches. A full picture of the orbital structure is then pieced together from the subsystem's 2-dimensional phase portraits on the branches together with fast transitions from the S-hysteresis' lower knee edge to its upper conductive branch and, similarly, from its upper knee to its primary conductive branch.

Here is a more detailed description of the illustration. Fig.10(a) shows the nullcline-surfaces in the $V_{\rm C}I_{\rm A}I_{\rm Na,p}$-state space. Because of the domination by K^+'s diffusive channel by condition (33), the intersection of the $V_{\rm C}$-nullcline surface and the $I_{\rm Na,p}$-nullcline surface, or the $V_{\rm C}I_{\rm Na,p}$-nullcline, on the primary conductive branch of Na^+'s IV-characteristic or the $I_{\rm Na,p}$-nullcline surface has a fold point, giving rise to one of the two necessary conditions for the K^+-mediated bursts. Because of the excitation condition (35), the $I_{\rm A}$-nullcline surface goes through K^+'s new diffusive dominating branch of the $V_{\rm C}I_{\rm Na,p}$-nullcline, giving rise to the other necessary condition for K^+-mediated bursts. Fig.10(b) is a zoom-in view on the effective region of spike-bursts. The condition (32) prevents any K^+-mediated burst from becoming a K^+-mediated action potential, circling around a would-be FitzHuge-Nagumo-like hysteresis on Na^+'s primary conductive branch like the case of Fig.9(a) if the condition (27) is not violated by condition (32). As a result, the burst continues, heading towards the lower knee edge of Na^+'s S-hysteresis. Once an orbit reaches the lower knee, it must jump upward to the upper conductive branch of the S-hysteresis. On the top branch and

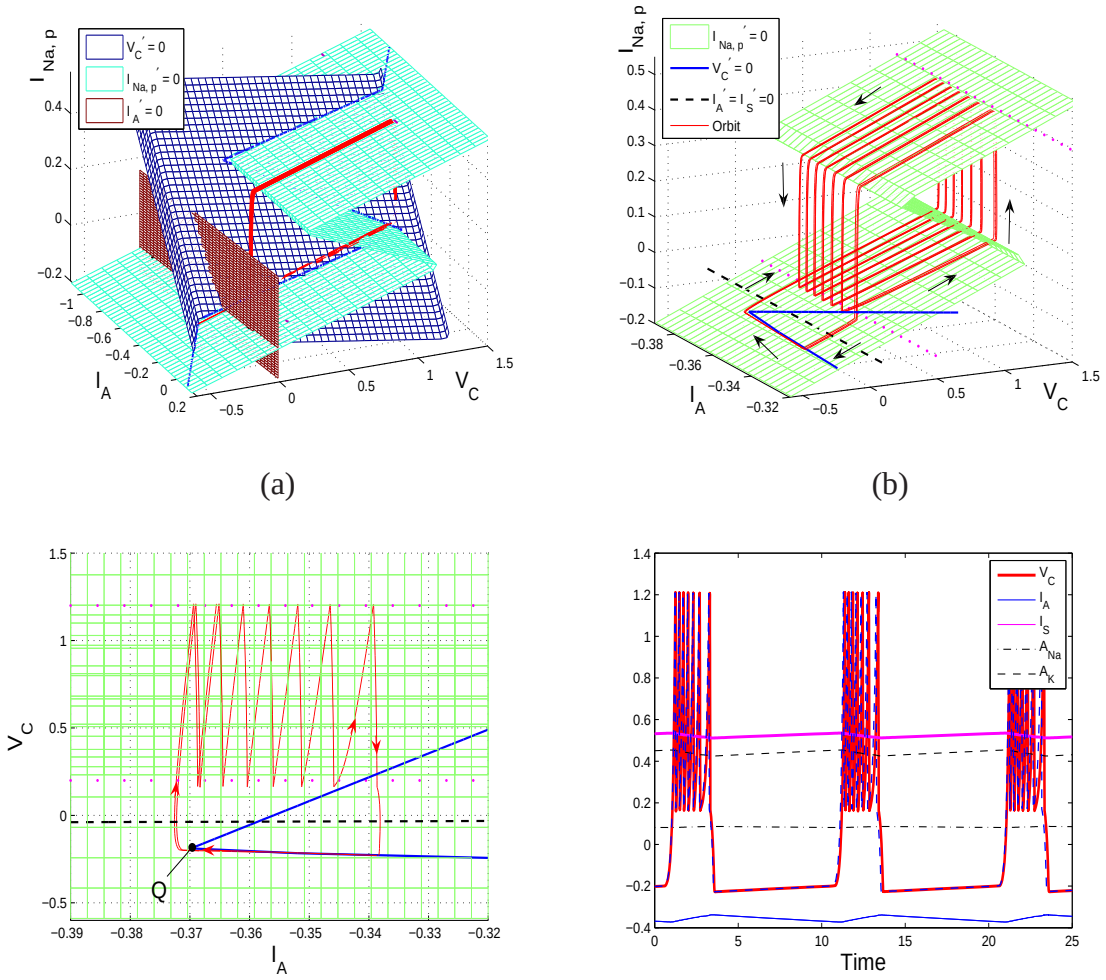

Figure 10: Na^+-K^+ spike-bursts. The same parameter values as Fig.8 except for $i_1 = 0.1,\ i_2 = 0.3$ for which the conditions (32, 33, 34, 35) are satisfied for Eq.(14). For consistence check, the dash spike-burst of (d) tracing the solid spike-burst in variable $V_{\rm C}$ is generated from circuit Fig.3(c)'s equations from Table 2 with exactly the same parameter values and initial conditions.

in the effective region shown, all solutions moves down ($V_{\rm C}{}' < 0$) in $V_{\rm C}$, up ($I_{\rm A}{}' > 0$) in $I_{\rm A}$, and towards the top knee of the S-hysteresis before falling from the edge down to the lower branch of the S-hysteresis. On the lower branch, solutions moves up in the $V_{\rm C}$-direction when in the region outside the fold of the $V_{\rm C}I_{\rm Na,p}$-nullcline ($V_{\rm C}{}' > 0$). Otherwise when inside the fold ($V_{\rm C}{}' < 0$), they move down in $V_{\rm C}$. Also, they move down in the $I_{\rm A}$-direction if in the region left of the $I_{\rm A}I_{\rm Na,p}$-nullcline ($I_{\rm A}{}' < 0$), and move up in $I_{\rm A}$ if otherwise ($I_{\rm A}{}' > 0$). Hence, the train of Na^+'-mediated spikes moves in the increasing direction of $I_{\rm A}$ when it is to the right of the $I_{\rm A}I_{\rm Na,p}$-nullcline and above the fold of the $V_{\rm C}I_{\rm Na,p}$-nullcline as shown. It will end upon entering the $V_{\rm C}I_{\rm Na,p}$-fold. The termination of spikes can also be taken as the end of the burst. However, once an orbit crosses into the left side of the $I_{\rm A}I_{\rm Na,p}$-nullcline ($I_{\rm A}{}' < 0$), another episode of spike-burst is set in motion, heading to the fold, turning around the fold, and heading to the lower knee edge of the S-hysteresis

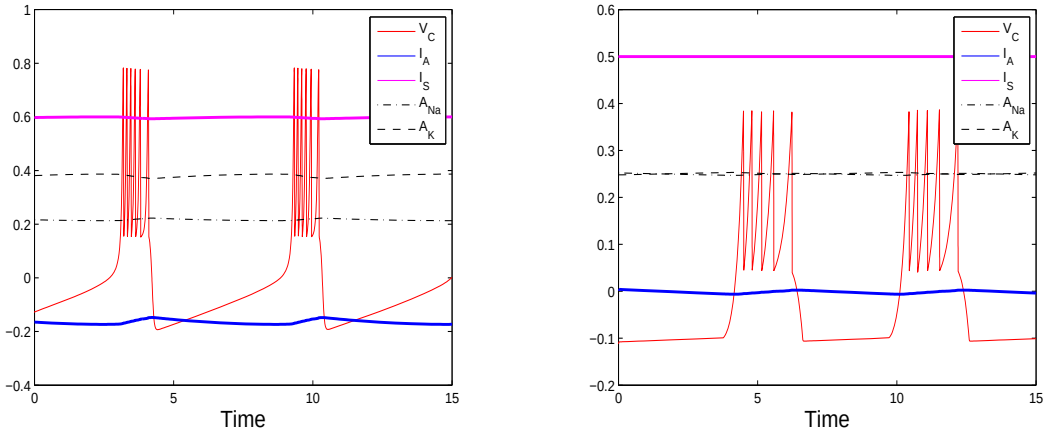

(a) (b)

Figure 11: (a) Simulation for Eq.(14) with smooth IV-curves of Table 3. Parameter values: $g_{\rm Na} = 0.2,\ d_{\rm Na} = -0.1,\ i_1 = 0.1,\ i_2 = 0.33,\ \bar{E}_{\rm Na} = 0.6,\ g_{\rm K} = 5,\ d_{\rm K} = -5.5,\ v_1 = 0.55,\ v_2 = 1.5, \bar{E}_{\rm K} = -0.7,\ C = 0.01,\ \lambda = 0.1,\ \gamma = 0.1,\ I_{\rm ext} = 0,\ \epsilon = 0.001$. (b) Simulation for the $\text{pNa}^+_+\text{sK}^+_-$ model from Table 2 with parameter values: $g_{\rm Na} = 1,\ d_{\rm Na} = -1.21,\ v_1 = -0.7,\ v_2 = -0.2,\ \bar{E}_{\rm Na} = 0.6,\ g_{\rm K} = 0.17,\ d_{\rm K} = -0.67,\ i_1 = 0.18,\ i_2 = 0.5, \bar{E}_{\rm K} = -0.7,\ C = 0.01,\ \lambda = 0.05,\ \gamma = 0.1,\ I_{\rm ext} = 0,\ \epsilon = 0.0005$.

again. Fig.10(c) shows the 3-dimensional $V_{\rm C} I_{\rm A} I_{\rm Na,p}$ phase portrait projected onto the $I_{\rm A} V_{\rm C}$-plane, and Fig.10(d) shows the time series of the spike-burst solution. Notice that the absolute ion pump current $I_{\rm S}$ oscillates in time as well.

Proposition 7. *The* $\text{pK}^+_-\text{sNa}^+_+$ *model can generate* Na^+-K^+ *spike-burst under the conditions (32, 33, 34, 35).*

3.7. Smooth IV-Curves. There are various ways to construct smooth IV-characteristic curves for both ions' passive channels. A brute-force way is just to approximate the piecewise linear curves $f_{\rm K}, h_{\rm Na}$ by polynomials of degree 3 and higher without decomposing them into their respective conductive and diffusive channels. Here instead we describe another systematic and direct way.

Take the N-shaped curve $I = f_{\rm K}(V)$ for example. It is simpler and more direct to specify instead the derivative $f_{\rm K}{}'(V)$ of the curve. Let $g_{\rm K}, d_{\rm K}, v_1 < v_2$ be the same parameters as above and assume the diffusive domination in $[v_1, v_2]$. Let $v_m = \frac{v_1+v_2}{2}$ be the middle point of the diffusive range. A $f_{\rm K}{}'(V)$ similar to the derivative of the piecewise linear curve satisfies the following:

(i) $V = v_1, v_2$ are the only critical point: $f_{\rm K}{}'(v_1) = f_{\rm K}{}'(v_2) = 0$.

(ii) Diffusion dominates the middle range $[v_1, v_2]$, with $d_{\rm K} + g_{\rm K} < 0$ being the combined maximal diffusive coefficient: $f_{\rm K}{}'(v_m) = d_{\rm K} + g_{\rm K}$.

(iii) Electromagnetic force dominates the range outside the interval $[v_1, v_2]$ with $g_{\rm K}$ being the saturated conductance: $\sup\limits_{-\infty<V<+\infty} f_{\rm K}{}'(V) = g_{\rm K} > 0$.

It is straightforward to check that the following form satisfies these conditions:

$$f_{\rm K}{}'(V) = \frac{|g_{\rm K} + d_{\rm K}|(V - v_1)(V - v_2)}{(\frac{v_2 - v_1}{2})^2 + \frac{|g_{\rm K} + d_{\rm K}|}{g_{\rm K}}(V - v_m)^2}.$$

Integrating the derivative gives the function

$$\begin{aligned} f_{\rm K}(V) &= \int_0^V f_{\rm K}{}'(v)dv \\ &= g_{\rm K}V + d_{\rm K}\mu\left[\tan^{-1}\frac{V - v_m}{\mu} + \tan^{-1}\frac{v_m}{\mu}\right], \text{ with } \mu = \frac{v_2 - v_1}{2}\sqrt{\frac{g_{\rm K}}{|g_{\rm K} + d_{\rm K}|}}, \end{aligned}$$

which is a canonical decomposition by defining $f_{\rm K}(V) = f_{\rm K,e}(V) + f_{\rm K,d}(V)$ with $f_{\rm K,e}(V) = g_{\rm K}V$ and $f_{\rm K,d}(V) = f_{\rm K}(V) - f_{\rm K,e}(V)$.

A function form for $h_{\rm Na}$ is similarly constructed from its derivative,

$$h_{\rm Na}{}'(I) = \frac{|\frac{1}{g_{\rm Na}} + \frac{1}{d_{\rm Na}}|(I - i_1)(I - i_2)}{(\frac{i_1 - i_2}{2})^2 + \frac{|\frac{1}{g_{\rm Na}} + \frac{1}{d_{\rm Na}}|}{\frac{1}{g_{\rm Na}}}(I - i_m)^2},$$

where $g_{\rm Na} + d_{\rm Na} > 0$ (equivalent to $1/g_{\rm Na} + 1/d_{\rm Na} < 0$) and $i_m = (i_1 + i_2)/2$. Both $f_{\rm K}$ and $h_{\rm Na}$ are listed in Table 3.

In fact, this is a general technique that can be used to generate the continuous piecewise linear IV-curves. For example, for the continuous piecewise linear functional $I = f_{\rm K}(V)$, its derivative at points other than the critical points v_1, v_2 is

$$f_{\rm K}{}'(V) = g_{\rm K} + d_{\rm K}(v_1 < V < v_2).$$

Imposing the continuity of $f_{\rm K}$ at the critical points to the integral $f_{\rm K}(V) = \int_0^V f_{\rm K}{}'(v)dv$ results in the functional we have been using.

Note that the configuration conditions (a,b,c,d) of the previous subsection are sufficient for spike-burst generation for the models with the piecewise linear IV-curves. However, they are not sufficient enough for the smooth IV-curves because unlike the linear case the critical points of the smooth curves will shift when combined in parallel. We will lose the precise strategic control on the locations of the new critical points. However, these conditions do give a good approximation of the new points that can lead us to the right nullcline configurations after a few trials-and-errors. Fig.11(a) is a Na^+-K^+ spike-burst simulation with the smooth IV-curves from Table 3.

3.8. $pNa^+_+sK^+_-$ Model Simulation. A $pNa^+_+sK^+_-$ model is exactly the same as the $pK^+_-sNa^+_+$ model except that K^+'s passive channel is a serial conductor-diffusor and Na^+'s passive channel is a parallel conductor-diffusor as illustrated in Fig.3(f). The polarities of the passive resting potentials and the directionalities of the ion pumps remain the same. The system of equations is listed in Table 2 with continuous piecewise linear functionals for both ions' passive channels as listed in Table 3. Fig.11(b) is a K^+-Na^+ spike-burst simulation of the $pNa^+_+sK^+_-$ model.

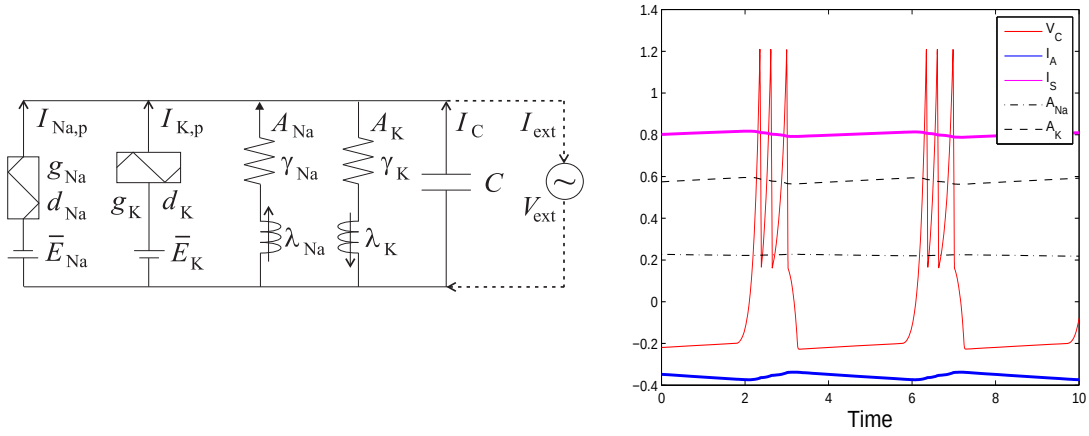

(a) (b)

Figure 12: (a) Circuit diagram for the $\mathrm{pK}^{+}_{-d}\mathrm{sNa}^{+}_{+d}$ type models whose equations are given by Eq.(36). (b) The same parameter values as Fig.10 except for $\gamma_{\mathrm{Na}} = 0.1,\ \gamma_{\mathrm{K}} = 0.05,\ \lambda_{\mathrm{Na}} = 0.05,\ \lambda_{\mathrm{K}} = 0.1$ for Eq.(36).

3.9. $\mathrm{pK}^{+}_{-d}\mathrm{sNa}^{+}_{+d}$ Model Simulation. With disjoint ion pumps, the pump parameter values $\lambda_{\mathrm{Na}}, \lambda_{\mathrm{K}}$ are not necessarily equal, nor are the parasitic resistances $\gamma_{\mathrm{Na}}, \gamma_{\mathrm{K}}$. The circuit equations corresponding to Eq.(13) become instead as below

$$\begin{cases} CV_{\mathrm{C}}{}' = -[I_{\mathrm{Na,p}} + f_{\mathrm{K}}(V_{\mathrm{C}} - \bar{E}_{\mathrm{K}}) + A_{\mathrm{Na}} - A_{\mathrm{K}} - I_{\mathrm{ext}}] \\ A_{\mathrm{Na}}{}' = \lambda_{\mathrm{Na}} A_{\mathrm{Na}}(V_{\mathrm{C}} - \gamma_{\mathrm{Na}} A_{\mathrm{Na}}) \\ A_{\mathrm{K}}{}' = -\lambda_{\mathrm{K}} A_{\mathrm{K}}(V_{\mathrm{C}} + \gamma_{\mathrm{K}} A_{\mathrm{K}}) \\ \epsilon I_{\mathrm{Na,p}}{}' = V_{\mathrm{C}} - \bar{E}_{\mathrm{Na}} - h_{\mathrm{Na}}(I_{\mathrm{Na,p}}). \end{cases} \tag{36}$$

Fig.12 shows a circuit diagram and a spike-burst simulation for this type of models.

3.10. Termination of Action Potentials and Spike-Bursts by Shutting Off Ion Pumps. Fig.13 shows typical dynamics regarding spike-bursts when one of the ion pumps in a $\mathrm{pK}^{+}_{-}\mathrm{sNa}^{+}_{+}$ model is blocked. When the Na^{+}-pump is shut off, the model reduces to a $\mathrm{pK}^{+}_{-}\mathrm{sNa}^{+}_{0}$ model, and the bursts persist. Thus, the Na^{+}-pump is not necessary. On the other hand, when the K^{+}-pump is rendered inoperable, all bursts are turned off, a typical outcome of $\mathrm{pK}^{+}_{0}\mathrm{sNa}^{+}_{+}$ models. Similar results are found from $\mathrm{pNa}^{+}_{+}\mathrm{sK}^{+}_{-}$ models and $\mathrm{pK}^{+}_{-d}\mathrm{sNa}^{+}_{+d}$ models. In terms of cellular metabolism, neuron's electrical pulses and spikes can be completely turned off by shutting down the intracellular ATPass.

Proposition 8. *To generate action potentials and spike-bursts, it is necessary to have one ion species to have parallel electro and diffusive channels and to have an ion pump at the same time.*

4. Discussions. We have described here a reductionistic approach to construct circuit models for neurons. Basic components include serial conductor-diffusors, parallel conductor-diffusors, and ion pumps. A minimal number of model parameters are summarized in Table 4. The parameter

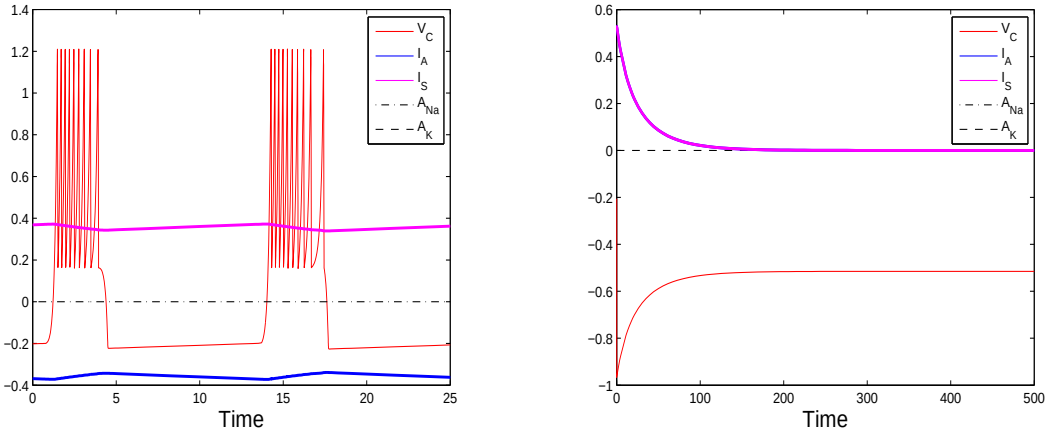

(a) (b)

Figure 13: Na^+-K^+ spike-bursts. The same parameter values as Fig.10 for Eq.(14). (a) The Na^+-pump is shut off with initial condition $A_{\rm Na}(0) = 0$ but $A_{\rm K}(0) > 0$. Spike-bursts persist. (b) The K^+-pump is shut off with $A_{\rm K}(0) = 0$ but $A_{\rm Na}(0) > 0$. Spike-bursts terminate.

list alone suggests that if the models are good approximations to real neurons then most of their structures but their passive resting potentials and their ranges of diffusion domination follow from circuit imperatives. The question of why those exceptional parameters become what they are is perhaps a question of evolution which certainly cannot be addressed here within the framework of circuitry.

Circuit properties of our pXsY models can be summarized and generalized as follows.

1. For cX^z_α models, where $z = +\ (\mathrm{resp.}\ -)$ if X^z is positive (resp. negative) charged, and $\alpha = +\ (\mathrm{resp.}\ -)$ if X^z is pumped outward (resp. inward), the active resting potential $E_{\rm X}$ and the passive resting potential $\bar{E}_{\rm X}$ must satisfy

$$0 < z\alpha E_{\rm X} < z\alpha \bar{E}_{\rm X}$$

   provided that $E_{\rm X}$ exists.

2. Ion X's passive resting potential is not stable in $\mathrm{cX}_\pm$ models but can be measured by the external current $I_{\rm ext}$ when other ions' currents are blocked and the membrane potential is clamped at zero $V_{\rm ext} = 0$.

3. The membrane resting potential $E_{\rm m}$ can be maintained at a fixed value in $\mathrm{cX}_\pm\mathrm{cY}_\mp$ models but with different ion pump currents for X and Y.

4. Action potentials mediated by ion X can be generated in $\mathrm{pX}_\pm\mathrm{yY}$ models only if X's diffusive channel can dominate all ions' conductive channels in parallel in a finite voltage range. Moreover, X-mediated action potential depolarizes (starts) most probably at a negative membrane potential.

5. Spike-bursts can be generated in $\mathrm{pX}_\pm\mathrm{sY}_*$ models only if ion X's diffusive channel can dominate all ions' conductive channels in parallel for burst generation

Table 4: Circuit Parameters

$g_{\rm J}$	max. conductance of ion J
$g_{\rm J}+d_{\rm J}$	max. diffusion coefficient for parallel conductor-diffusors
$g_{\rm J}d_{\rm J}/(g_{\rm J}+d_{\rm J})$	max. diffusion coefficient for serial conductor-diffusors
$\bar{E}_{\rm J}$	passive resting potential
$E_{\rm J}$	active resting potential with $E_{\rm J}=\frac{g_{\rm J}}{g_{\rm J}+1/\gamma_{\rm J}}\bar{E}_{\rm J}$
$(v_1+\bar{E}_{\rm J}, v_2+\bar{E}_{\rm J})$	diffusion dominating voltage range for parallel channels
(i_1, i_2)	diffusion dominating current range for serial channels
$\gamma_{\rm J}$	ion pump resistance of ion J
$\lambda_{\rm J}$	ion pump coefficient of ion J in the unit of $1/[\mathrm{ampere}\cdot\mathrm{Henry}]$
C	membrane capacitance

and ion Y's diffusive channel can dominate its conductive channel or other ion's conductive channel in series for spike generation.

6. Action potentials and spike-bursts may not be generated in $\mathrm{pX_0sY_*}$ models which do not have an ion pump or only have an inoperable ion pump for ion X.

The model, the analysis, and the result can be extended in many ways. In one aspect, the conductive branches need not symmetrically have the same maximum conductance for the S-curve, nor for the N-curve. Also, the IV-characteristic curves for passive channels need not be either piecewise linear or smooth, but can be a mixture of both. In another aspect, additional ion channels can be incorporated into the minimal two-ions models as pointed out in Sec.2. In fact, all the simulations above were actually done for a corresponding $\mathrm{pXsYcCl}_0^-$ model with $g_{\rm Cl}=0.01,\ d_{\rm Cl}=0,\ \bar{E}_{\rm Cl}=-0.6$, but the smallness in magnitude of the conductance and diffusion parameters did not qualitatively change the dynamics of the minimal models. It is conceivable that some nontrivial extensions may alter the minimal channel structures described here in some fundamental ways that are not yet understood. We also note that most of the results on action potential and spike-burst generations have been obtained for the $\mathrm{pK}_-^+\mathrm{sNa}_+^+$ models. Similar work is yet to be done for the $\mathrm{pNa}_+^+\mathrm{sK}_-^+$ models.

We have categorized some basic dynamical behaviors of the models as summarized above. Yet there are some more features left unexplored. The existence of a junction-fold point leading to a period-doubling cascade ([5, 6, 11]), the existence of Shilnikov's orbit ([7]), and the existence of a chaotic attractor with a canard point ([9], but for a smooth S-hysteresis only) are distinctive possibilities for our models because our models and the food chain models cited in the references share a fundamentally similar geometry for the said phenomena. However, these features may not be as prominent as the three kinds analyzed above for neural dynamics.

We have given a general yet design-specific method to construct neuron models. Given the multitude, flexibility, and robustness in choosing the ion species in a model, the serial/parallel

configurations of the ion channels, the individual shapes of the IV-characteristics of the passive ion channels, the functional characteristics of ion pumps, and the parameter values, one should be able to use our method to customize a model to fit a particular type of neurons.

We anticipate little difficulty to implement the models in real circuits. This is especially true for circuit Fig.3(d) with a linear inductor with constant inductance L. (The simulations of Fig.10 and Fig.11 demonstrated that $I_{\rm S}$ is approximately constant, implying that $L = 1/(\lambda I_{\rm S})$ can be fixed at a constant as well.) Electronic devices with S-hysteresis and N-hysteresis are almost as common as other elementary components of resistors, inductors, and capacitors. For example, a tunnel diode has an N-shaped IV-characteristic like our parallel conductor-diffusor. The middle negative resistive region of a tunnel diode is the result of quantum tunneling by which electrons can cross an energy barrier because the probability, by means of the electron's wave function, to find them in the classically forbidden side is substantial. An S-characteristic can be constructed by flipping and rotating an N-characteristic, and the necessary operations can be easily implemented by elementary circuit networks ([2]). The only non-standard component for our circuit models is the one-way ion pump whose characteristic is given by (1). But there should be no practical difficulty to realize the characteristic by some circuit network. However, there is a good reason to have a simpler, stand-alone component for the ion pump because it is the key to the neural metastability and plasticity to be discussed in [12].

Acknowledgement: Special thanks to Jack Hale and Shui-Nee Chow who believed in the project in its inception when the outcome was nothing but uncertain.

References

[1] Chay, T.R. and J. Keizer, *Minimal model for membrane oscillations in the pancreatic beta-cell*, Biophys J., **42**(1983), pp.181-190.

[2] Chua, L.O., Introduction to Nonlinear Circuit Theory, McGraw-Hill, New York, 1969.

[3] Deng, B., *A mathematical model that mimics the bursting oscillations in pancreatic β-cells*, Math. Biosciences, **119**(1993), pp.241–250.

[4] Deng, B., *Constructing homoclinic orbits and chaotic attractors*, Int. J. Bif. & Chaos, **4**(1994), pp.823–841.

[5] Deng, B., *Glucose-induced period-doubling cascade in the electrical activity of pancreatic β-cells*, J. Math. Bio., **38**(1999), 21–78.

[6] Deng, B., *Food chain chaos due to junction-fold point*, Chaos, **11**(2001), 514–525.

[7] Deng, B., G. Hines, *Food chain chaos due to Shilnikov orbit*, Chaos, **12**(2002), 533–538.

[8] Deng, B., G. Hines, *Food chain chaos due to transcritical point*, Chaos, **13**(2003), 578–585.

[9] Deng, B., *Food chain chaos with canard explosion,* Chaos, **14**(2004), 1083–1092.

[10] Deng, B., *Equilibriumizing all food chain chaos through reproductive efficiency,* Chaos, **16**(2006), 043125(7 pages), DOI: 10.1063/1.2405711.

[11] Deng, B., I. Loladze , *Competitive coexistence in stoichiometric chaos,* Chaos, **17**(2007), 033108(14 pages), DOI: 10.1063/1.2752491.

[12] Deng, B., *Neural metastability and plasticity mediated by two ion pump,* preprint, (2007) (http://www.math.unl.edu/∼bdeng1/Papers/DengNeuralMetaStability.pdf)

[13] FitzHugh, R., *Impulses and physiological states in models of nerve membrane,* Biophy. J., **1**(1961), pp.445–466.

[14] Fonseca, J., S. Kaya, S. Guennoun, and R. Rakowski, *Temporal analysis of valence & electrostatics in ion-motive sodium pump,* J. Comp. Elec. DOI 10.1007/s10825-006-0141-3.

[15] Hindmarsh, J.L. and R.M. Rose, *A model of neuronal bursting using three coupled first order differential equations,* Proc. R. Soc. Lond. B. **221**(1984), pp.87–102.

[16] Hodgkin, A.L. and A.F. Huxley, *A quantitative description of membrane current and its application to conduction and excitation in nerve,* J. Physiol. **117**(1952), pp.500–544.

[17] Kandel, E.R., J.H. Schwartz, and T.M. Jessell, Principles of Neural Science, 3rd ed., Elsevier, 1991.

[18] Kaya, S., personal communication, 2007.

[19] Keener, J.P., *Analog circuitry for the van der Pol and FitzHugh-Nagumo Equations,* IEEE Trans. on Systems, Man, and Cybernetics, **13**(1983), pp.1011–1015.

[20] Morris, C. and H. Lecar, *Voltage oscillations in the barnacle giant muscle fiber,* Biophysical J., **35**(1981), pp.193–213.

[21] Nagumo, J., S. Arimoto, and S. Yoshizawa, *An active pulse transmission line simulationg nerve axon,* Proc. IRE, **59**(1964), pp.2061–2070.

[22] Rakowski, R.F., S. Kaya, and J. Fonseca, *Electro-chemical modeling challenges of biological Ion pumps,*J. Comp. Elec. **4**(2005), pp.189-193.

[23] Rinzel, J., *A formal classification of bursting mechanisms in excitable systems,* in Teramoto E., Yamaguti, M.(eds) Mathematical topics in population biology, morphogenesis, and neurosciences, Lect. Notes Biomath., Vol. 71, Springer 1987.

[24] Zigmond, M.J., F.E. Bloom, S.C. Landis, J.L. Roberts, and L.R. Squire, Fundamental Neuroscience, Academic Press, 1999.